PSEUDOATROPHY OF THE BRAIN IN MULTIPLE SCLEROSIS: THE EFFECT OF
THERAPY ON $T_1$ MEASURES OF BRAIN WATER CONTENT

by

EMILIE CESCHI MACKIE

B.A., DARTMOUTH COLLEGE, 2007

A THESIS SUBMITTED IN PARTIAL FULFILLMENT OF THE REQUIREMENTS FOR
THE DEGREE OF

MASTER OF SCIENCE

in

THE FACULTY OF GRADUATE STUDIES

(Experimental Medicine)

THE UNIVERSITY OF BRITISH COLUMBIA

(Vancouver)

June 2010

*Abstract*

Magnetic Resonance Imaging (MRI) measures of $T_1$ relaxation provide a sensitive and reproducible measure of water content in vivo. In the present study $T_1$ histograms were used to monitor changes in the brain water content of multiple sclerosis (MS) patients initiating Disease Modifying Therapies (DMT). The initiation of DMT, which target inflammation, is associated with a decrease in brain volume (BV) greater than would be expected by natural history alone. Reductions in BV may reflect worsening disease in untreated patients; however for patients treated with DMT, reductions in BV early in the treatment course may represent a clinical improvement due to initial anti-inflammatory effects of therapy and the resulting decrease in edema. The initial change in BV upon starting DMT is termed **pseudoatrophy,** a reversible decrease in BV due to a loss of water from the brain parenchyma. Patients with clinically definite MS planning on initiating DMT were recruited and scanned at two time points prior to initiating therapy and two time points after initiating therapy to determine the change in water content of the brain.

## *Table of Contents*

## *List of Tables*

## *List of Figures*

## List of Symbols and Abbreviations

| | |
|---|---|
| **2D** | Two Dimensional |
| **3D** | Three Dimensional |
| **BV** | Brain Volume |
| **BPF** | Brain Parenchymal Fraction |
| **BPV** | Brain Parenchymal Volume |
| **CIS** | Clinically Isolated Syndrome |
| **CNS** | Central Nervous System |
| **CSF** | Cerebrospinal Fluid |
| **DMT** | Disease Modifying Therapy |
| **EDSS** | Expanded Disability Status Scale |
| **$F_w$** | Water fraction |
| **GM** | Gray Matter |
| **γ** | Gyromagnetic Ratio |
| **IFN** | Interferon |
| **ISF** | Interstitial Fluid |
| **J** | Proton's Angular Momentum |
| **MHz** | MegaHertz |
| **M-3** | Month Minus 3 |
| **M0** | Month 0 (baseline) |
| **M3** | Month 3 |
| **M6** | Month 6 |
| **MS** | Multiple Sclerosis |

| | |
|---|---|
| **MRI** | Magnetic Resonance Imaging |
| **NAWM** | Normal Appearing White Matter |
| **NMR** | Nuclear Magnetic Resonance |
| **PNS** | Peripheral Nervous System |
| **PPMS** | Primary Progressive Multiple Sclerosis |
| **PRISMS** | Prevention of Relapses and Disability with Interferon beta 1a Subcutaneously for Multiple Sclerosis |
| **RRMS** | Relapsing Remitting Multiple Sclerosis |
| **SPMS** | Secondary Progressive Multiple Sclerosis |
| **T** | Tesla, unit of magnetic field strength |
| **$T_1$** | Spin-Lattice Relaxation Time |
| **$T_1$WI** | $T_1$ Weighted Imaging |
| **$T_2$** | Spin-Spin Relaxation Time |
| **$T_2$WI** | $T_2$ Weighted Imaging |
| **TE** | Echo Time |
| **tiw** | Three Times (or Thrice) Weekly |
| **TR** | Repetition Time |
| **μ** | Magnetic Momentum |
| **WM** | White Matter |

## *Acknowledgments*

First of all I would like to thank my supervisor Dr. Anthony Traboulsee who was always calm when I was not. Thanks also to my committee David Li, Alex MacKay and Helen Tremlett who provided valuable guidance and insight.

I have been fortunate to work with an amazing group of people whose help, empathy and sense of humor were greatly appreciated. Special thanks to Dr. Irene Vavasour who patiently showed me the ropes and helped me work through numerous mini crises. I am also deeply grateful to Dr. Corree Laule who read every word of this thesis (some of them twice), saved me from a rogue manhole and has been an amazing role model and friend throughout my time at UBC. I also enjoyed time with Linda Chandler and Roger Tam, segmentation parties with Madeleine Hodgson and Sandra Meyers, late nights in the lab with Saeed Kalantari and Davis Holmes and statistical consultations with YinShan Zhao.

A special thanks to Trudy, Paul, Linda, and the staff at the UBC MRI Research Center for their expertise and for the many great conversations. This study would not have been possible without their contributions.

I am eternally grateful to the individuals who volunteered for this study. Spending time with them has been my great privilege.

Finally, I truly appreciate the funding from the Multiple Sclerosis Society of Canada, without which this project could not have been realized.

*"In examining disease, we gain wisdom about anatomy and physiology and biology. In examining the person with the disease, we gain wisdom about life."*

- Oliver W. Sacks

## *Dedication*

*To my family for their love and support and to my partner Bevan who lived the bachelor life with twice as many dishes for the last months of this thesis.*

## 1.  Introduction

Multiple Sclerosis (MS) is a progressive inflammatory neurological disease of unknown origin and is the leading cause of neurological disability in young Canadian adults.[1] Magnetic Resonance Imaging (MRI) is one of the most important clinical and research tools available for the diagnosis and monitoring of MS in Canada, and worldwide.[2] MRI measures of brain volume (BV) have been proposed as one of the best in vivo measures of neuro-degeneration in MS patients and have emerged as important predictors of disease progression in MS.[18-19, 24]

The rate of BV loss has been shown to predict subsequent disability progression and is a promising biomarker for clinical trials to examine the effect of disease modifying therapies (DMT). Loss of BV in MS is generally considered to be due to cellular atrophy occurring as a result of disease activity which results in permanent tissue loss. Brain atrophy is a decrease in BV caused by the irreversible loss of central nervous system (CNS) tissue due to a pathological process arising from MS. In MS research the terms "brain volume loss" and "brain atrophy" are often used interchangeably however many mechanisms other than tissue damage and tissue loss contribute to BV changes in MS. Changes in tissue edema and cellular infiltrates may also affect measures of BV. **Pseudoatrophy** is a phenomenon that has been observed in clinical trials of DMT in MS.[3] For the purpose of this study pseudoatrophy is defined as reversible changes in BV caused by shifts in brain water content. Pseudoatrophy may mask the beneficial effects of treatment in preventing tissue loss and has implications for the usefulness and reliability of monitoring BV changes in clinical trials and clinical practice.

## 1.1.     *Multiple Sclerosis: Disease and Significance to Canadians*

MS is a complex demyelinating disease of the CNS which is most often diagnosed in young adults, with the first clinical manifestations appearing between ages 10 and 50.[4] MS affects twice as many women than men with a significantly higher incidence of the disease in temperate climates compared to warmer ones. MS is also more prevalent in Northern European Caucasians than other ethnic groups. Canadians have one of the highest rates of MS in the world with a prevalence of 24 cases per 10,000.[1] MS is the leading cause of non-trauma related disability in young Canadians.[1]

The causes of MS remain unknown. Like many other neurological and auto-immune disorders MS likely involves several different genetic and environmental factors. In families with an affected member, the risk is 3-5%, with the risk rising to approximately 34% for the monozygotic twin of an affected patient, strengthening the notion of a genetic component to the disease. Environmental components may include Vitamin D (sunlight), infections, smoking and many others.[1]

Clinically Isolated Syndrome (CIS) is the earliest stage of MS in which patients present with a single attack of neurological symptoms, but often with multiple lesions already visible on the initial brain MRI.[5] Lesions are patches of inflammation in the CNS in which the neurons have been stripped of their myelin.[6] MS can attack any area of the CNS; therefore the signs and symptoms can be diverse. Among the most common clinical symptoms are numbness and tingling, weakness, optic neuritis and dizziness.[4] More difficult to quantify are cognitive symptoms such as fatigue, slowed thinking, altered mood etc.

MS is characterized by several different subtypes. Approximately 85% of patients initially present with relapsing–remitting MS (RRMS)[4] which involves recurrent episodes of neurological symptoms (relapses) followed by periods of recovery. Relapses involve an acute onset of symptoms (over hours or days), which gradually resolve. Attacks (relapses) can last anywhere from days to months and between attacks, symptoms may resolve completely; however, permanent neurological problems often occur, especially in later stages of the disease.[4] Later in the course of the disease, about 50% of cases evolve into secondary-progressive MS (SPMS). SPMS is characterized by worsening symptoms and progressive disabilities which occur with or without relapses. Approximately 10% of people with MS initially present with a progressive form of the disease known as primary progressive MS (PPMS) where patients grow gradually worse without experiencing remissions.[4] Currently there is no cure for MS although the use of DMT has been moderately effective. The MS Society of Canada estimates the cost of MS to the Canadian economy to be more than $1 billion per year.[1]

## *1.2.    Magnetic Resonance Imaging (MRI)*

MRI is an indispensable diagnostic tool. It is non-invasive, high resolution and can generate thin-section images of the human body from any angle. Unlike other imaging techniques, MRI does not expose patients or research subjects to x-rays or radiation but rather takes advantage of a magnetic field and radio waves to produce signals that are reconstructed on a computer. The application of MRI to the CNS has improved the ability to diagnose and monitor pathology in the brain and spinal cord.

MRI is an imaging technique derived from the principles of Nuclear Magnetic Resonance (NMR). Atoms consist of a nucleus and orbiting electrons. NMR exploits magnetic nuclei (nuclei with an odd number of protons or neutrons) such as H, P, Na etc. The hydrogen nucleus (also called proton) precesses about its axis which generates a large magnetic moment. The magnetic moment arises from the nuclear spin. When this moment is placed in a magnetic field, it causes the nucleus to undergo precession, similar to a top in a gravitational field. The frequency of this precession is called the Larmor frequency and is proportional to the magnetic field strength. Each proton acts as a weak magnet and possesses a magnetic moment $\mu$, as defined in the equation below:

$$\mu = \gamma \mathbf{J}$$

where $\gamma$ is the gyromagnetic ratio (42.58 MHz/Tesla) and $\mathbf{J}$ is the proton's angular momentum.[7] In addition to hydrogen, other nuclei with angular momentum equal to or greater than ½ possess a magnetic moment.[7] These nuclei (spins) act like tiny magnets and they will align in a strong, constant magnetic field. Radiofrequency (RF) fields are used to systematically knock the spins off the alignment of this magnetization, causing the nuclei to produce a signal detectable by the scanner. The frequency depends on the strength of the static magnetic field and the nuclei of observation. The energy given off at a specific resonance frequency can be detected and used to gather information about the nuclei their surroundings. This signal can be manipulated by additional magnetic fields to build up enough information to construct an image of the brain.

In a strong magnetic field, the magnetic moment of protons, which are ordinarily distributed in random directions, align. When a patient is placed in the magnetic field of an

MRI scanner their protons align parallel with the main magnetic field and anti-parallel to it. The aligned position is slightly favored as the nucleus is at lower energy in this position. Applying an RF pulse (at the Larmor frequency for hydrogen) causes protons to absorb energy and tips the magnetization vector away from its initial direction. These RF pulses are usually applied through a coil. MRI scanners also have three gradient magnets arranged in the x, y and z directions inside the main magnet which can manipulate the main magnetic field and encode spatial information.[7] After excitation the nuclei try to return back to their lowest energy state, or equilibrium state, via a process called relaxation. During relaxation when the hydrogen protons return to alignment the main magnetic field they release energy. This energy's signal is picked up by the coil and sent to a computer. The computer system receives the data that can be converted to an image using a Fourier transform.

Relaxation involves two processes longitudinal relaxation and transversal relaxation.[7] $T_1$ describes the time needed for the spins to restore their longitudinal relaxation. $T_2$ describes the speed with which spins lose their transverse magnetization.[7]

## 1.2.1. $T_1$

The $T_1$ relaxation time or longitudinal (spin-lattice) relaxation time is a measure of how quickly the nuclei realign with the external field. The rate at which protons return to the equilibrium state is related to the size of the molecules or the lattice to which they are bound. As the protons return to alignment the longitudinal magnetization increases until it returns to its original value. $1/T_1$ is also called longitudinal relaxation rate and is proportional to 1/(water content).[8]

## 1.2.2.    $T_2$

$T_2$ describes the transverse relaxation time. After the RF pulse protons begin to lose phase coherence and transverse magnetization decreases. Protons are influenced by their neighboring nuclei and these internal magnetic field variations are distinctive for different tissues.

## 1.2.3.    MRI Contrast

$T_1$ and $T_2$ are influenced by tissue composition, structure and surroundings (differences in proton density). In many diseases the pathological process results in changes of the water content, and this is reflected in the MR image. $T_1$ is longer at stronger field strengths because it takes more energy to align protons.[7]

By choosing different combination of imaging parameters we can obtain images with different contrast. $T_1$-weighted images are based on differences in $T_1$ characteristics between tissues, $T_2$ weighted images are influenced by differences in $T_2$. In standard spin-echo MRI sequences, different repetition time (TR, time between each RF excitation), and echo time (TE, waiting time before the MR signal is recorded) will result in images with a different degree of $T_1$ and $T_1$ weighting or contrast.[7] Inversion recovery pulse sequences are used to give images heavy $T_1$-weighting, they can provide strong contrast between tissues having different $T_1$ relaxation times.

Conventional MRI sequences are routinely used in the diagnostic workup and monitoring of patients with MS. The standard MRI protocol for diagnosing MS includes a sagittal fast FLAIR (fast fluid-attenuated inversion-recovery), axial fast spin echo (FSE) PD/$T_2$ (PD: long

TR, short TE) ($T_2$: long TR long TE), axial pre-gadolinium $T_1$ ($T_1$: short TR, short TE), $3DT_1$ and an axial gadolinium-enhanced $T_1$.[6, 9] These techniques provide a sensitive measure for visualizing MS lesion load and changes over time. Conventional imaging can also monitor BV in MS non-invasively. However conventional MRI techniques are not specific to the diverse pathological features of inflammation, demyelination, axonal loss, gliosis and atrophy in MS and are often insensitive to subtle changes that may affect BV. $T_1$ relaxation time provides a quantitative MR parameter to investigate water content, which is involved in BV changes.

## 1.2.4.    *MRI Measurements of Brain Volume as a Biomarker of Neuro-degeneration*

BV loss due to MS can be monitored using cross-sectional studies by comparing with age-matched healthy controls or in longitudinal studies with serial scans from the same subjects. BV changes occur over a relatively short period of time (one year or less) and most MRI scanners can provide good and consistent data for analysis.[10] Brain atrophy can be identified qualitatively and quantitatively from images by recognition of an increase in CSF spaces [11] and MRI measurements of BV are the main tool used to measure changes in brain atrophy in living patients with MS.

Loss of BV due to MS can be measured in several ways. There is a large range of techniques available for the measurement of BV, including 2D and 3D techniques as well as regional and global measures.[10, 12-15] Each MRI technique provides quantitative estimates of BV and progressive changes in BV. There are techniques that measure global atrophy as well as regional atrophy that focus on a specific region of the brain, such as the corpus

callosum. Measurement of change within these focal areas may have a further advantage because of the greater degree of change in proportion to the rest of the brain.[16]

3D techniques provide quantification of whole BV and studies suggest this may better reflect global disease effects.[12] However global measures may miss atrophy that only impacts specific regions. Segmentation of 3D methods can be used to quantify the individual volumes of grey matter, white matter, and cerebrospinal fluid compartments.[12] Each of these BV techniques has unique strengths and weaknesses, and the reliability of the information that can be obtained is dependent on image quality. The most important features of any MRI atrophy index are reproducibility, sensitivity to change and stability over time.

### 1.2.5. MRI Techniques for Investigating the Mechanisms of Pseudoatrophy

Monitoring BV changes in MS lacks pathologically specificity. To be useful as a biomarker for neurodegeneration and irreversible disability, it is necessary to separate the amount of irreversible change due to atrophy (tissue loss) from the reversible change due to pseudoatrophy. The main goal of this thesis was to measure shifts in brain water content.

To investigate the theory that changes in water content is the mechanism underlying pseudoatrophy; a reproducible method of measuring water content is needed. MRI is able to provide a quantitative in vivo approximation of brain water content. A variety of imaging techniques have been used for this purpose. The cellular make-up and the water content of brain tissue influences both $T_1$ and $T_2$ times and both allow for measures of brain water

content. Changes in $T_1$ have been used to investigate edema and have been found to closely mirror changes in tissue hydration.[17]

### 1.2.5.1.  $T_1$ MRI Water Content Measures

Water is present in the brain in bound and free forms. Free water has a long relaxation time; bound water's relaxation time is much shorter. The measured longitudinal relaxation time, $T_1$, is a weighted average of the "free" and "bound" water. "Bound" water represents water in tissue of the body that is bound to macromolecules or organelles. Therefore it is motion restricted and had a much shorter relaxation time than free water.

Pathological processes can affect $T_1$ relaxation time in the brain parenchyma. $T_1$ increases as water in the tissue becomes less organized and more mobile.[18] $T_1$ and water content are related ($1/T_1$ is proportional to 1/(water content)).[8]

Fatouros at al. investigated the sensitivity of MR relaxation times to changes in water content in vivo.[8] The method involved creating $T_1$ maps from five phase-sensitive inversion recovery MR images and was validated in phantom experiments and in vivo using feline and human biopsy tissue.[19]

$T_1$ is the local tissue longitudinal relaxation time and $F_w$ = (water weight/total brain weight). In the Fatouros study the $F_w$ was measured using gravimetrically obtained values of corresponding tissue acquired via biopsy. The calculated $T_1$ values were shown to correlate with the MRI $T_1$ map.[8] From the $T_1$ map, a "water map" was calculated using an equation derived from the fast exchange two-state model ($1/F_w = A + B/T_1$). The accuracy of the $F_w$ determination was dependent on the accuracy of the measured $T_1$ values. Absolute $F_w$ values

can be extracted from the water maps; and histogram analysis can be conducted and compared. A histogram of an image is a plot of the number of pixels with a given data value.

There are limitations to using a $T_1$ technique to measure water content. $T_1$ does not equal water content and the correlation is imperfect. While we assume that changes in $T_1$ will represent changes in water content, other factors can affect $T_1$ signal for example iron can shorten $T_1$.[20]

## 1.3.    *Brain Volume*

The CNS is made up of the brain, optic nerves and spinal cord. The spinal cord relays sensory and motor information between the peripheral nervous system (PNS) and the brain. The brain controls simple motor behaviors, such as breathing but also elaborate cognitive behaviors such as learning and memory.[21]

The human brain weighs approximately 1500 grams and accounts for 2% of body weight.[2] The BV of healthy humans varies from 1000-2000 ml with an average volume of 1350- 1400 ml.[21] The brain is a heterogeneous environment that contains neurons, glia, axons, myelin, blood vessels and CSF. The brain is made of soft tissue and the water content in normal brain tissue has been measured by spectroscopy to fall between 0.68 in the WM and 0.80 in the GM of healthy human adults.[21, 22] The fundamental components of the CNS are the neurons and glia. Neurons are highly specialized electrically excitable cells that process and transmit information by chemical and electrical signaling. Neurons have dendrites for receiving signals, a cell body to integrate information and an axon to propagate the signal to the next neuron via the synapse. The neuronal axons fill the majority of the space in the brain.

Signal transmission is accelerated up to 50 times by the myelin sheath, a lipid bilayer that is wrapped around segments of the axon by the processes of oligodendrocytes (a type of glial cell).[2] Myelin provides insulation to the axons which inhibits charge leakage through the axonal membrane therefore action potentials.[21] In myelinated axons, action potentials do not propagate as waves, but jump along the axon at the nodes of Ranvier (gaps between the myelin sheath). Glia are also critical in the human brain, performing structural, metabolic, developmental and immunological functions. The typical human brain contains roughly 16-33 billion neurons with glia outnumbering neurons roughly four to one.[21] Axons wrapped in myelin projections from oligodendrocytes encompass the white matter (WM) for the brain; the neuronal cell bodies compose the grey matter (GM).[21] Other cellular components include the cells that make up the choroid plexus and the meninges. In addition to cells the cranial cavity contains four major fluid compartments: the blood that flows through the entire brain structure; the interstitial fluid (ISF) that bathes neurons and glia; the CSF, which circulates in the brain ventricles and surrounds the spinal cord; and the intracellular fluid.[21, 23] Materials present in ISF and CSF can freely diffuse between these two compartments.[21, 23]

The CSF is produced by the choroid plexus and maintains a constant external environment for the cells of the CNS.[21, 23] It also provides a mechanical cushion to protect the brain from impact. Elements of BV that may be influenced by the MS disease state and treatment are the neurons, glia and fluid compartments.


## 1.4.    *Human Water Regulation*

The regulation of water homeostasis in the human body is crucial. Water comprises approximately 60-70% of human body weight and the water content of the body can fluctuate

on the order of 3% of total body weight.[24] Total body water is distributed between the intracellular fluid and the extracellular fluids.

## 1.4.1. Water in the Body

The human organism is composed of trillions of cells. Cells require a constant environment to survive: water, oxygen, glucose, ions and cellular waste.[25] The human body maintains a tightly regulated concentration of solutes and water to maintain the cells.

Most biological membranes are semi-permeable, permeable to water but not aqueous solutes. Water can flow across membranes from compartments of lower concentration to areas of higher concentration.[25] Osmolality is the concentration of all solutes in a given weight of water and osmoregulation is the active regulation of the osmotic pressure of bodily fluids to maintain the homeostasis of the human body's water content. Homeostasis keeps the body fluids from becoming too dilute or too concentrated.

Water metabolism is the balance between the intake and excretion of water. Water intake comes from the content of ingested food and beverages. Water loss from the body occurs in a variety of ways, via the kidney, the respiratory system, and the skin.[26] Two major mechanisms for regulating water metabolism are thirst and pituitary secretion of the hormone vasopressin.

## 1.4.2. Water in the Brain

Under normal physiologic conditions the brain preserves BV through tightly controlled homeostasis. Several mechanisms are responsible for the maintenance of brain homeostasis

during short-term fluid shifts including angiotensin, vasopressin and aquaporin channels.[23, 27]

Precise regulation of brain water content and by relation BV is crucial to normal function in the CNS.[28] The brain is occupied by neurons surrounded by glia with the remaining extracellular space filled with fluid.[29] Small water content changes in extracellular space can affect ion concentration and neuronal function.[27] Mechanisms for water transport across plasma membranes play a central part in healthy brain physiology. It is likely that these mechanisms are also important in pathophysiological processes like edema.

The BBB acts as a "pure" lipid membrane which forms a diffusion barrier. Water must cross directly through the membranes of the endothelial cells by dissolving in the lipids.[23] Angiotensin and vasopressin two of the hormones involved in the regulation of the systemic fluid and electrolyte metabolism in the body may also act within the CNS and contribute to regulating brain water content.[30]

Aquaporins are a family of water channels that have been found to facilitate trans-membrane transport of water in a number of organs including the brain.[27] The discovery of aquaporins in the brain has changed the understanding of water fluctuations in the CNS. Water does not simply move throughout the brain via the lipid bilayer. Water shifts in the brain are regulated by a sophisticated network of membrane proteins with water-selective pores.[27]

Aquaporin 4 is the principal aquaporin found in the brain: mostly in the plasma membrane and astrocytes. It has also been suggested that aquaporin 4 plays a part in the development of the BBB.[27, 31] It is likely that aquaporin 4 primarily serves to mediate activity-dependent water fluxes that are required to maintain ion and volume homeostasis at central synapses.

Water transport in the brain is not solely the domain of aquaporins. Brain vasculature is uniquely adapted to increase water permeability when subjected to osmotic stress and this may be regulated by vasopressin or angiotensin.[28] However, the aquaporins are the primary regulators because of their capacity and selectivity for water transport.

### 1.4.2.1.  Brain Volume Modifiers

Possible modifiers of BV include physiological and pathological factors, and BV shifts may be transient or permanent. Hydration status, alcohol, and diet are the main physiological factors that have been shown to influence BV [21, 32, 33]; dehydration may lead to shrinkage of astrocytes (glial cells crucial for water regulation between the cellular, vascular and ventricular compartments of the brain). BV shifts have also been observed in individuals with anorexia nervosa where studies suggest that a decrease in serum proteins causes fluid shifts and a decrease in synaptogenesis leading to decreases in BV.[32]

Another factor that may contribute to an increase or decrease in BV is the level of hydration at the time of the MRI. A study by Duning et al. found that lack of fluid intake prior to an MRI scan can lead to a transient, reduction in BV similar in degree to that seen annually from MS disease progression.[24]  The results suggested that unless fluid intake of a patient is controlled in a way that ensures an equivalent level of hydration prior to different scans, it was a possible source of variation in BV. However the UBC MRI Research Center recently completed a similar study with contradictory findings.[34] The study involved 20 healthy subjects between the ages of 18-55 scanned four times in a 3T scanner at various levels of hydration. The results of this study demonstrated no statistical differences in brain water content at different states of hydration [34] using two different independent techniques. Brain

homeostasis for water content is tightly controlled under normal or moderate fluctuations in general body hydration could explain these results. It is possible that more extreme degrees of hydration or dehydration might produce different results.

Elements of BV that may be influenced by the MS disease state and treatment are the neurons, glia and fluid components. BV may also be affected when the blood brain barrier (BBB) is diffusely compromised, resulting in brain edema; a state of increased brain water content.[21, 35] Brain edema arising from disease can be localized or generalized. There are two types of edema in the brain: 1) cytotoxic edema which results from damage to neurons and glia, leading to a buildup of sodium and water inside the cells and 2) vasogenic edema which results from an influx of water across the BBB into the extracellular space.[36]

Patients with MS exhibit an overall increase in total brain water of approximately 2.2%, compared with normal individuals.[37] Inflammation can have a significant impact on edema formation,[38] so the increase in total brain water in patients with MS could be due, at least in part, to diffuse low-grade inflammation causing mild brain edema, although this is yet to be proven. Inflammation-induced breakdown of the BBB is thought to play a key role in the uptake of fluid by the brain.[39] The BBB may be disturbed in all lesions and at all stages of MS (active, inactive, lesions, Normal Appearing White Matter (NAWM), etc). The observation the NAWM appears to have higher water content than normal WM in unaffected individuals further supports the relationship between inflammation and diffuse low grade edema in MS.[40] Monitoring changes in BV has practical applications for detecting therapeutic outcomes and disease specific prognosis.

## 1.5.    Brain Atrophy

BV has become an important measurement in the study of neurodegeneration and MRI is an increasingly important diagnostic and research tool for investigating volume-related brain changes. MRI techniques can detect volumetric changes as small as 1.5 to 3 ml or 0.2-0.13% of total BV,[24] thereby allowing researchers to examine and quantify slight fluctuations in BV. Many neurological and psychiatric disorders such as Alzheimer's disease, epilepsy, MS and schizophrenia exhibit regional and/or global neuro-anatomical changes.[41-43] The rate of global brain atrophy observed in healthy subjects is much lower than in those with disease [9, 11, 39, 44-48] and it is also important to differentiate between pathologic rates of atrophy from normal age-related atrophy.[33]

## 1.6.    Multiple Sclerosis as a Model of Brain Atrophy

MS is characterized by multifocal recurrent episodes of autoimmune mediated inflammation. Acute inflammation and edema are accompanied by different degrees of demyelination, destruction of oligodendrocytes and may be followed by remyelination, axonal loss and/or gliosis.[36] Reductions in brain and spinal cord volume have been recognized as common pathological features in MS. Studies in patients with CIS have found that BV loss occurs early in the disease process.[11] BV is inversely related to the disease duration of MS.[47, 48] As MS progresses, reductions in BV become more widespread, affecting more regions of the CNS. Studies indicate that BV changes occur over a relatively short period of time at a rate of 0.6-1.35% loss of BV annually in patients with RRMS.[49] Similar rates of BV loss have been reported in patients with SPMS and PPMS.[47, 48] Rates of BV loss in

cross sectional studies of healthy controls have studies have reported annual decreases of 0.1–0.3% decrease in BV which is significantly lower than rates seen in MS.[50] WM and GM atrophy are also common pathological features in MS.[9]

### *1.6.1.     Mechanisms of Brain Atrophy in Multiple Sclerosis*

Loss of BV in MS is generally thought to be due to atrophy occurring as a result of disease activity causing permanent tissue loss. The loss of myelin, which is the classical feature of MS lesions, results in a loss of tissue and contributes to atrophy. However it is clear that many other processes are involved in BV loss.[3] The etiology and mechanisms of atrophy in patients with MS are poorly understood but thought to be multi-factorial. (Figure 1-1).
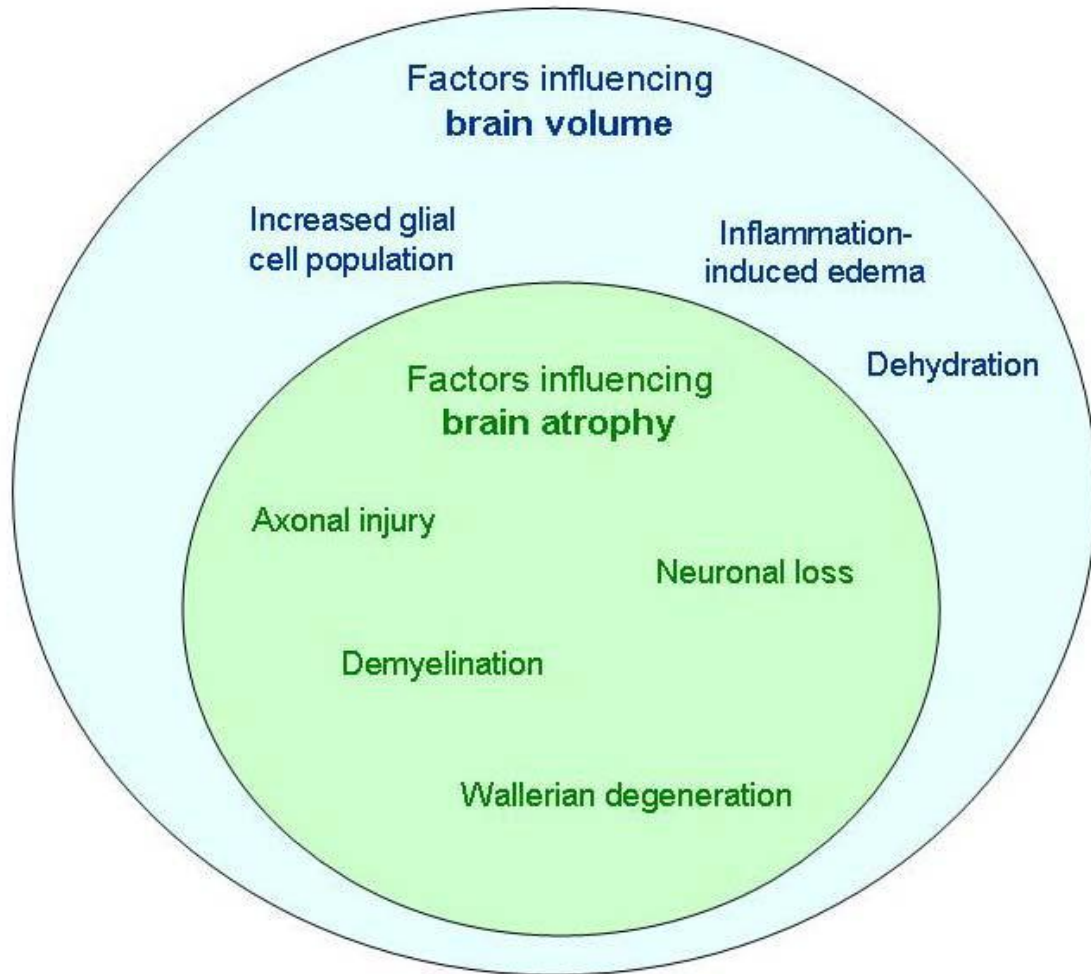
**Figure 1-1 Factors contributing to changes in BV and brain atrophy in patients with MS**

Demyelination, axonal damage, neuronal loss, and Wallerian degeneration are thought to be the major contributors to the pathologic atrophy associated with MS and chronic outcomes of the inflammatory phase of the plaque or disease process. Edema caused by inflammation appears to be one of the main factors that confound the relationship between brain volume and atrophy.

Axonal damage and loss has been observed in pathological studies of active inflammatory lesions.[14] Demyelination, axonal damage, neuronal loss, and Wallerian degeneration are thought to be the major contributors to the pathologic atrophy associated with MS [12, 39, 51] with each of these features being chronic outcomes of the inflammatory phase of the plaque or disease process.

Contrast enhancing lesions reflect the acute inflammatory step in lesion development. MRI markers of inflammation (Gadolinium-enhancing lesions, new and enlarging $T_2$-hyperintense lesions) are only partially predictive of subsequent BV loss in patients with MS.[38] Evidence indicates that a compartmentalized component of inflammation exists that is not easily detected by conventional MRI which may independently contribute to neurodegeneration and thus brain atrophy.[40]

The pathologies underlying atrophy are multi-factorial and may not be constant over time.[39] These pathologies differentially affect gray and white matter, and regional versus global CNS.[52] Understanding how these pathologies appear in neuroimaging can help us better understand atrophy and design outcome measures for clinical trials.

Tissue damage and subsequent atrophy are not the sole factors that affect the BV of patients with MS. In MS BV is primarily affected by three mechanisms: fluctuations in edema (associated with disturbances of the BBB and inflammation); tissue loss of myelin, axons and other glial cells, and regeneration (remyelination).[3, 14]

Non-inflammatory processes may also contribute to MS related atrophy. These include growth factor depletion, impaired electrical conduction, and pathologic iron deposition,

leading to loss of WM and grey matter GM tissue. [40] The complete set of mechanisms contributing to progressive tissue loss and atrophy is still under investigation.

Focal brain edema is also associated with new lesion development. MS lesions have minimal mass effect and it is unlikely that individual lesions would have a major impact on total BV measures. Although both GM and WM are affected by MS, higher levels of inflammation are detected in regions of WM than in GM.[49] Reductions in BV due to white matter atrophy could be masked, to some extent, by inflammation-associated edema in these areas.[53] This may also apply to GM, although inflammation is usually not a feature of cortical lesions.[46, 54]  Results from a 3-year longitudinal study in patients with CIS suggestive of MS also support this hypothesis of diffuse inflammation and edema.[46] In patients who had developed MS by the end of the study, WM lesion loads increased considerably during the 3-year observation period. However, WM fractional volume did not decrease accordingly, and results even suggested a small increase in mean WM fractional volume during the study (+1.3%). In contrast, mean GM fractional volume decreased significantly (−3.3%) over 3 years.[46]  The authors attributed this observation to the influence of diffuse inflammation and glial cellularity, which may have offset the loss of BV caused by loss of parenchymal components.[4]  Microglial activation appears to be present in the NAWM of the majority of patients with MS.[55] The implication of these findings is that diffuse edema may mask the severity of brain atrophy in MS.

### 1.6.2. Natural History and Significance of Brain Atrophy in Multiple Sclerosis

Brain atrophy has been reported as a feature of MS in early pathological studies.[39] In MS **brain atrophy** is defined as an irreversible decrease in BV due to the pathological loss of brain tissues that reflects the cumulative loss of neurons, axons, myelin and glia particularly oligodendrocytes.[12, 56] CNS atrophy is a multifactorial process that occurs early in the disease and measurable changes in brain and spinal cord volume have been demonstrated over periods as short as 6-12 months.[57] As the disease progresses, reductions in BV become more widespread, affecting all regions of the brain (Figure 1-2),[58] and impacting on both gray and white matter compartments.[12] It has been established that monitoring brain atrophy in MS is a valuable biomarker for irreversible disease.[59]

BV is an important measurement because it correlates more closely with the level of patient disability than lesion volume or activity measures.[9, 39] The "clinical-imaging paradox" of MS describes the discrepancy between lesion burden seen on MRI and clinical findings. Overall, changes in BV have a higher correlation with clinical disability as measured on the Expanded Disability Status Scale (EDSS) and changes in EDSS than other conventional cerebral lesion measures, such as $T_1$ hypointense and $T_2$ hyperintense lesions volume.[57, 60] Longitudinal studies have shown that brain atrophy is a significant predictor of subsequent long term neurological deterioration.[58] Therefore, loss of BV has been widely adopted as a useful biomarker of disease progression or neurodegeneration in clinical trials of MS treatments.

Measures of regional atrophy are useful specifically in helping to understand cognitive dysfunction and other clinical findings. Studies have linked many of the common spheres affected by MS such as cognition, mood, fatigue and quality of life, with changes in BV.[58, 60] Zivadinov and colleagues noted that the rate of BV loss correlated with both cognitive dysfunction and physical disability.[9] and ventricular enlargement has also been connected with cognitive dysfunction.[58]

In the past 20 years MRI has assumed a prominent role in the diagnosis and monitoring of the evolution of MS in vivo. MRI is instrumental in monitoring the appearance and evolution of pathology, some of which might not be clinically apparent.[9] Lesions are the most visible pathology seen on MRI; however it is clear that the pathology of MS is far more complex than lesion quantification and volume. Destructive or degenerative changes associated with axonal loss are common in MS.[61]. In addition there is evidence that brain atrophy is not restricted to later stages of MS. Unlike other MRI markers, such as lesion load, BV measures can be directly correlated to MS disease duration.[39, 51, 60, 62] Brain atrophy becomes widespread as the disease progresses, affecting all brain regions including all the cerebral lobes, the compact WM tracts, brainstem and cerebellum.[40] BV loss is seen in all clinical subtypes of MS.[37, 60] (Figure 1-2)
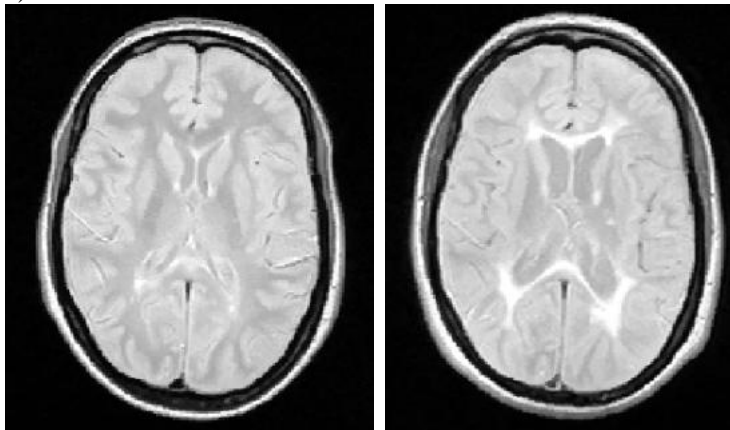
a)
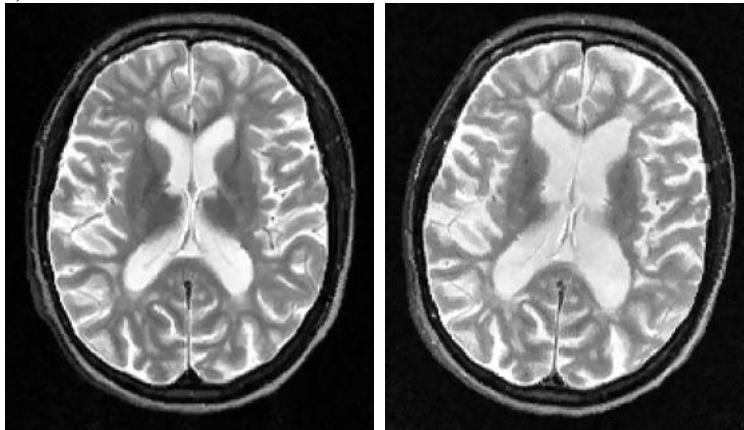


BPV at baseline: 0.663          BPV at year 8: 0.588

b)



BPV at baseline: 0.780          BPV at year 8: 0.651

**Figure 1-2 Magnetic resonance imaging (MRI) scans showing progression of brain atrophy in MS**

Magnetic resonance imaging (MRI) scans showing progression of brain atrophy in multiple sclerosis (MS) in patient in the Prevention of Relapses and Disability by Interferon beta-1a Subcutaneously in Multiple Sclerosis (PRISMS) study with long-term follow up. Patients had a standardized MRI at baseline and with the same scanning parameters and accurate repositioning at the year 8 long-term follow up visit. a) 11.8% decrease in brain parenchymal volume (BPV) between baseline and year 8 on $T_2$ weighted scan; b) 16.5% decrease in BPV from baseline to year 8, and ventricular enlargement on proton density (PD) scan.[63]
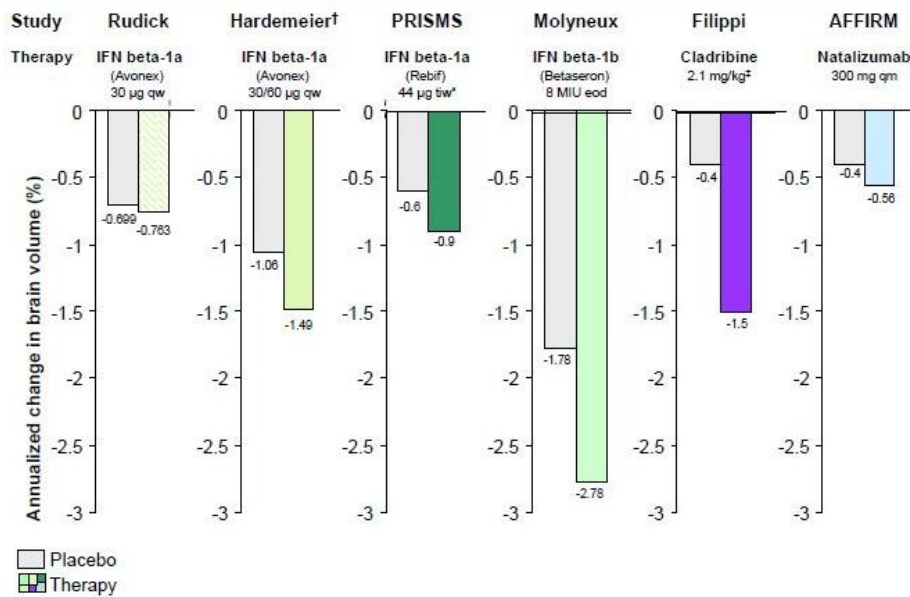
## 1.7.    *Disease Modifying Therapy*

There is no cure for MS; however several therapies have proved effective at promoting rrecovery of function after an attack, preventing future attacks, and postponing disability.[64] The term DMT includes five anti-inflammatory, immunomodulatory and immunosuppressive treatments that are currently available including IFN beta. IFN beta is a common treatment for patients with RRMS; it is aimed at reducing the biological activity of MS in order to prevent or postpone future neurological injury.

### 1.7.1.    *Evidence for Pseudoatrophy Induced by Multiple Sclerosis Therapies*

DMT can affect physiological mechanisms and produce reversible decreases in BV. In MS patients BV is primarily affected by three mechanisms: inflammation and edema (changes in water content), tissue loss (myelin, axons, glial cells) and regeneration (remyelination).[65] Edema caused by inflammation is one of the main factors that confound the relationship between BV and atrophy. However, treatments that target inflammation are the principal therapeutic strategy for most patients with MS. Therefore, while reductions in BV may reflect worsening disease in untreated patients, for treated patients, reductions in BV early in the treatment course may even represent a clinical improvement due to initial anti-inflammatory effects of therapy and the resulting decrease in edema. On examination of BV data from clinical studies of DMTs that target inflammation, this is exactly the observed pattern (Figure 1-3)**.**

a)



| Study | Rudick | Hardemeier† | PRISMS | Molyneux | Filippi | AFFIRM |
|-------|--------|-------------|--------|----------|---------|--------|
| Therapy | IFN beta-1a (Avonex) 30 µg qw | IFN beta-1a (Avonex) 30/60 µg qw | IFN beta-1a (Rebif) 44 µg tiw* | IFN beta-1b (Betaseron) 8 MIU eod | Cladribine 2.1 mg/kg‡ | Natalizumab 300 mg qm |

Placebo
Therapy

*IFN beta-1a 22 µg tiw also investigated in PRISMS study; ‡Cladribine 0.7 mg/kg also investigated; †Placebo' value shows mean change in brain volume in 3 months prior to starting active treatment. NB: Changes in brain volume are not comparable across trials due to differences in MRI analysis techniques and patient populations.
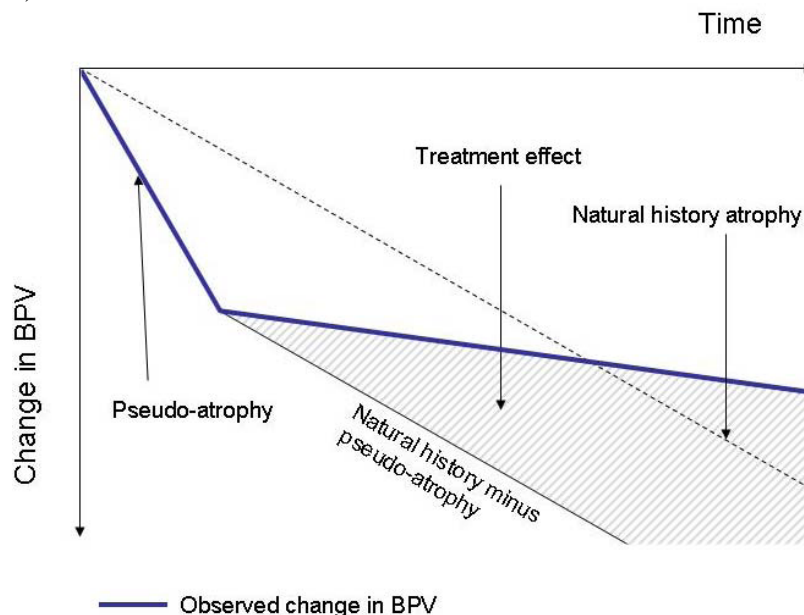
b)



Observed change in BPV

**Figure 1-3 Early changes in BV following initiation of treatment with DMT**

a) Early changes in brain volume following initiation of treatment with disease-modifying therapies in six studies in multiple sclerosis: annualized mean percentage change in brain volume from baseline.[12, 16, 53, 57, 61]; b) A theoretical graph showing typical changes in brain parenchymal volume (BPV) in patients with MS after treatment with DMT (thick line). This graph is based on observations made in a large number of clinical trials for MS treatments. The use of natural history data to compensate for pseudoatrophy is also illustrated.

A study investigating the efficacy of IFN beta-1a (30 mcg once weekly) in patients with RRMS reported similar reductions in BPF for active treatment and placebo groups during the first year.[66] However, during the second year of the study, the rate of BPF reduction was significantly less in the treatment arm than in the placebo arm.[66] IFN beta-1a is known to have effects on disease activity and disability progression in the first year of treatment and, therefore, it is unlikely that the observed trend in BPF was due to delayed therapeutic effect. The initial masking of decelerated atrophy by the BV loss due to reduced inflammation and associated edema (pseudoatrophy) could explain the apparent lack of benefit in terms of BPF during the first year of treatment. However, this study was confounded by the decrease in the number of subjects who completed the second year of the study.

Another study investigated changes in BPF in patients with RRMS, before and during treatment with IFN beta-1a 30 mcg once weekly.[67] There was no placebo group and therefore the annualized rate of BV change was estimated using three monthly MRI's before and after initiating therapy. The relative annualized rate of BPF reduction increased significantly from −1.06% before treatment to −1.49% during the first 4 months of treatment, which may reflect the initial reduction in inflammation due to the drug. The annualized rate of BPF reduction then decreased significantly to −0.33% over the subsequent 32 months of treatment, which may reflect the benefits of treatment in terms of reduced atrophy. The main limitation of this study was the lack of a concurrent placebo group. However, it does provide insight into the timing of the pseudoatrophy effect and a potential strategy for future therapeutic trials.

The PRISMS (Prevention of Relapses and Disability with Interferon beta 1a Subcutaneously in Multiple Sclerosis) study investigated the effects of IFN beta-1a (22 or 44 mcg three times weekly (tiw)) in patients with RRMS and measured changes in BPV over a period of 8 years.[63] In the first 2 years of the study, patients were randomized to IFN beta-1a 22 or 44 mcg tiw, or placebo and the rate of BPV loss in the IFN beta-1a 44 mcg tiw group was greater than that observed in the placebo group.[63] After 2 years, patients receiving placebo were re-randomized to active treatment (late-treatment group) and the blinded study continued for a further 4 years. After re-randomization to active treatment, the placebo group had a similar initial BPV loss seen in the original 44 mcg tiw group. Furthermore, over the course of treatment the rate of BPV loss decreased, and during the 4–8 years after treatment was initiated, the rate of BPV loss in the IFN beta-1a 44 mcg tiw group was lower than that seen in the placebo group during the first two years of the study (years 0–2 in late treatment group).[63] Again, it is difficult to calculate the on treatment rate of tissue loss related to disease progression (atrophy) since the initial BV used for that calculation has been affected by pseudoatrophy. Not only does pseudoatrophy mask potential therapeutic benefit on this outcome, it can also exaggerate the magnitude of actual tissue loss. If the pseudoatrophy effect plateaus early after treatment, then subsequent BV changes would primarily reflect tissue loss.

The IFN beta-1b study for the treatment of secondary progressive MS also demonstrated a greater decrease in BV in a subset of the original patients. During the first 6 months of the study, the treated group had a decrease of -1.39% compared to placebo group decrease of -0.89%. However, the decrease from baseline to month 24 was -2.17% for the IFN beta-1b group versus -2.76% for the placebo group.[68] It is unlikely that this early greater decrease in BV while starting therapy is clinically detrimental as overall, the treated cohort fared better

clinically in terms of delaying disability progression compared to placebo. Although most of the data published on BV reductions with initial treatment are from studies of IFN beta-1a, evidence for inflammation-related effects on BV has also been observed with other treatments for MS. Two studies have reported BV changes during methylprednisone treatment used to control acute relapses in patients with RRMS.[69, 70] Both studies found a rapid reduction in BV within the first month of treatment, and this effect slowed over subsequent months. The rapid and significant reduction of BV seen in these patients may reflect the high levels of inflammation present during an MS exacerbation. In one study in patients with PPMS treated with IV cladribine, there was a marked effect on the prevention of new inflammatory lesions on MRI.[71] In addition, there was a greater degree of BV decrease at the end of the 12-month, double blinded study in the treated patients compared with placebo.[71] This may reflect a greater reduction of diffuse inflammation with a potent anti-inflammatory medication, reflected in the greater BV losses.

In an 18-month trial evaluating glatiramer acetate (GA) treatment in patients with RRMS, the placebo and GA groups showed similar levels of BV loss during the first 9 months of treatment. However, in the second 9 month period a significantly greater reduction in BV was observed in the placebo group compared to the GA group.[72, 73] Assuming that MS treatments have a beneficial effect on tissue loss, then the inability to detect this benefit in the first year on treatment could either be due to several mechanisms. Pseudoatrophy may exaggerate the rate of tissue loss relative to a placebo group or tissue loss occurs months to years after the injury and so a treatment started today may not prevent an established process of tissue loss. Until we can separate pseudoatrophy from true tissue loss, it will be difficult to

use MRI measures of BV to explore the mechanism of action of new or current therapies on the pathogenesis of atrophy.

Similar treatment-induced, reversible BV decreases have been seen with other therapies for other indications, including renal dialysis[74] and valproic acid treatment for localization-related epilepsy.[75] Interestingly, increases in BV related to therapy have also been reported,[76] providing yet another potential confounder in the interpretation of a stabilization in BV changes in future clinical trials. There have been no studies demonstrating a reversal of pseudoatrophy due to the MS therapies mentioned previously.

The long term benefits of the currently approved DMTs for MS still generate debate.[77] However there is no clinical evidence that these treatments are neurotoxic or that pseudoatrophy is associated with tissue loss in addition to a reduction in edema. While some formulations of IFN beta (Betaseron, Fiblaferon, BG9015) have shown neurotoxicity at high doses in patients with malignant gliomas, neurotoxicity has not been reported for IFN beta treatment in patients with MS. Moreover, there is some evidence to suggest IFN beta may even provide a degree of neuroprotection. Indirect evidence of neuroprotection comes from studies with other MRI biomarkers including the assessment of chronic $T_1$ weighted black holes.[78-80] Neurotoxicity is an important consideration in the development of any new therapeutic strategy for MS.

## 1.8.     Aims, Objectives, Hypothesis

The goal of this thesis is to determine the effect of high dose, high frequency interferon therapy for the treatment of MS on $T_1$ measures brain water content within 6 months of

starting treatment. By measuring $T_1$ water content prior to initiation of therapy and during therapy we hope to track changes caused by the DMT. **Our hypothesis is that brain water content (measured by $T_1$) will decrease after initiating DMT.** We believe these shifts in water content are responsible for the BV changes related to pseudoatrophy. The main focus of this research project is to better understand the physiologic mechanisms underlying pseudoatrophy as well as establishing sound methodology to investigate them.

## *1.9.       Motivations*

MRI is one of the most important clinical and research tools available to diagnosis and monitor MS in Canada and worldwide. Clinicians and researchers are increasingly dependent on quantitative measurements derived from MRI data both for the development of new therapies and monitoring their impact on the overall disease course. Despite a vast amount of research in MS, the relationship between tissue degeneration and clinical disability is still not well understood, and the correlation between MRI biomarkers and clinical symptoms is modest at best. For this reason, precision and accuracy are of utmost importance when performing studies to evaluate treatment protocols with an acute awareness of potentially confounding factors such as changes in water content with treatment. This knowledge will lead to better designed clinical trials and more efficient development of effective new treatments. A better understanding of how water content impacts the MR measures can be used in developing and monitoring new therapies for MS.

## 2. Materials and Methods

### 2.1.      Subjects

This study is supported by the MS Society of Canada and was reviewed and approved by the University of British Columbia Clinical Research Ethics Board. A total of 30 MS subjects diagnosed with clinically definite MS, eligible for DMT (at least two relapses in the past two years) and planning on initiating therapy with "high dose" IFN (interferon beta 1a (22 to 44 mcg SC tiw) and interferon beta 1b 250 mcg SC EOD) are being recruited at the UBC Hospital MS Clinic. Once recruited, subjects are initiated on IFN therapy per routine clinical practice at UBC. This involved a dose escalating titration schedule over 8 weeks. The concurrent use of over the counter oral analgesic medications for flu like side effects was not restricted. If a patient required the use of high dose oral or intravenous steroids for a MS relapse, the MRI scan was performed prior to the use of steroids as it could affect the primary outcome brain water content (and BV). All subjects had a diagnosis of MS and were able to provide informed consent.  We required that subjects be aged between 18 and 55 years of age so BV loss would not occur as a result of the normal ageing process. Signed informed consent was obtained prior any evaluations.

Study exclusion criteria included: No subject who had taken high dose oral or intravenous steroids within 30 days. No use of interferons, copaxone, imuran or experimental treatment within the past 6 months and no use of mitoxantrone or cyclophosphamide within the past 12 months. Patients who were unable to provide informed consent, unable to tolerate the MRI protocol or any contra-indications to MRI were not recruited to the study.

## 2.2. Study Protocol

The study protocol involved 4 MRI scans performed over the course of 8-9 months (Table 2-1). Pre-treatment scans included scans one and two Scan one occurred 1 to 3 months prior to initiating treatment (Month -3). The second scan was scheduled to coincide with the initiating of treatment (Baseline: Month 0). Scans three and four (post-treatment scans) were acquired three months and six months following initiation of treatment (Month 3 and Month 6). By month 3 patients were taking the full dose of IFN. The Month -3 and baseline (Month 0) MRI scans were used as control to measure the natural progression of atrophy and $T_1$ prior to treatment initiation. The scans taken at months 3 and 6 were be used to determine the effects of therapy on brain water content and BV compared to baseline. The study did not delay therapy as it often takes patient in British Columbia three to six months to begin treatment.

**Table 2-1 The timeline of the Pseudoatrophy study**

| Scan Number | Scanning Time | Timeline |
|:---:|:---:|:---|
| 1 | 1 hour | Month -3 to -1: Screening scan prior to starting IFN beta |
| 2 | 1 hour | Month 0: Baseline, upon initiation of IFN beta |
| 3 | 1 hour | Month 3: after starting IFN beta |
| 4 | 1 hour | Month 6 after starting IFN beta |

.

## *2.3.     MRI Scan Protocol*

All MRI scans were performed on a Philips 3.0 T Achieva system (Philips Medical System, Best, The Netherlands) using a phased-array head coil and Dual Nova gradients. The scans were acquired in the axial plane using the Genu and Splenium of the corpus callosum as reference for accurate repositioning (Figure 2-1)**.**
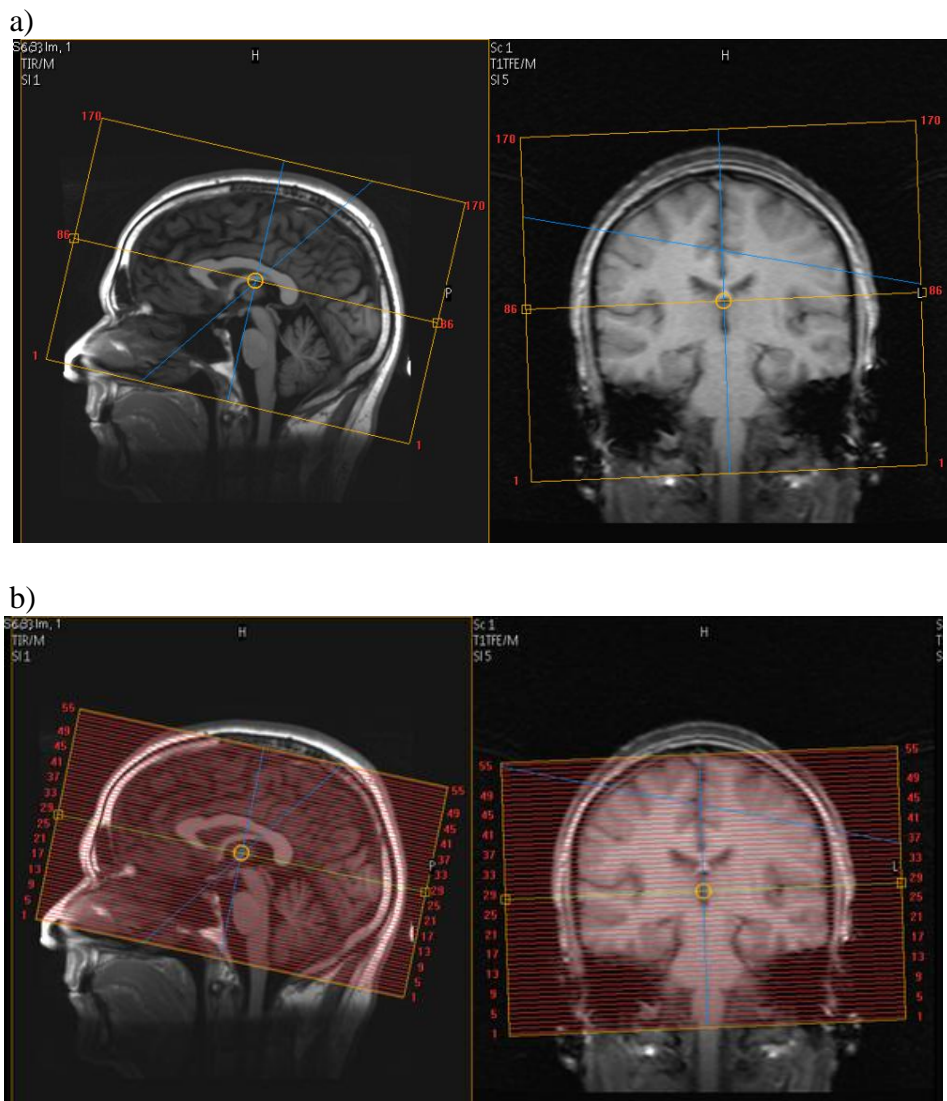
a)



b)



**Figure 2-1 Location of MRI scans**
a) Alignment of $3DT_1$ scans using the genu and splenium of the corpus callosum.
b) Alignment of inversion recovery $T_1$ scans using the genu and splenium of the corpus callosum.

Following a quick $T_1$-weighted survey for patient positioning and a reference scan, a true-midline $T_1$ inversion recovery (IR) sagittal scan (1 slice, TR = 1900 ms, TI = 800 ms, TE = 10 ms, slice thickness = 4 mm) and a FLAIR (fluid-attenuated inversion-recovery) (29 slices, TR = 11000 ms, TE =125 ms, IR 2800 ms, slice thickness = 5 mm) were collected. The slices were positioned using the bottom edge of bottom slice positioned using the corpus callosum as a reference.

An $IRT_1$ ($T_1$ inversion recovery sequence) (5 TIs (150 – 2100 ms), TR/TE=8/4.6 ms, TFE = 100, shot interval = 3000 ms, FA = $12^o$, 55 slices) was also collected. Additional scans included a 3D $T_1$-weighted scan positioned to include 4-6 slices above the brain (170 slices, TR = 7.8 ms, TE = 3.6 ms, Flip Angle 8°,TFE factor 200 and a voxel size of 1x1x1cm) .

## 2.4.    MRI Analysis and Post Processing

### 2.4.1.    Registration

Images were exported from the scanner as Philips PAR/REC files. All images were converted to NIfTI format using FSL version 4.1.4. FSL is a comprehensive library of analysis tools for FMRI, MRI and DTI brain imaging data (FMRIB's Diffusion Toolbox, FMRIB Software Library, www.fmrib.ox.ac.uk).

All images were registered to the M-3 TI = 1200 ms scan using the FSL (FMRIB's Linear Image Registration Tool (FLIRT) version 5.5). $T_1$ images were registered with transformation type (Model/DOF) restricted to traditional 9 parameter model. In the advanced options the initial optimization search stage was performed with  the x, y, z set with the angular range at max: 15° and min: -15°, a mutual information cost function with 32 histogram bins, SINC

interpolation was used in the final re-slice transformation. Following the registration process all images were inspected visually to ensure proper alignment.

### *2.4.2.    Segmentation*

WM and whole brain segmentation were accomplished using FSL FAST and eroding by one pixel to minimize partial volume. We obtained the MRI parameters for both white matter and full brain parenchyma (CSF removed). Segmented masks were created for each subject from scan 1 (Month -3) (Figure 2-2). All masks were inspected visually to ensure proper segmentation.
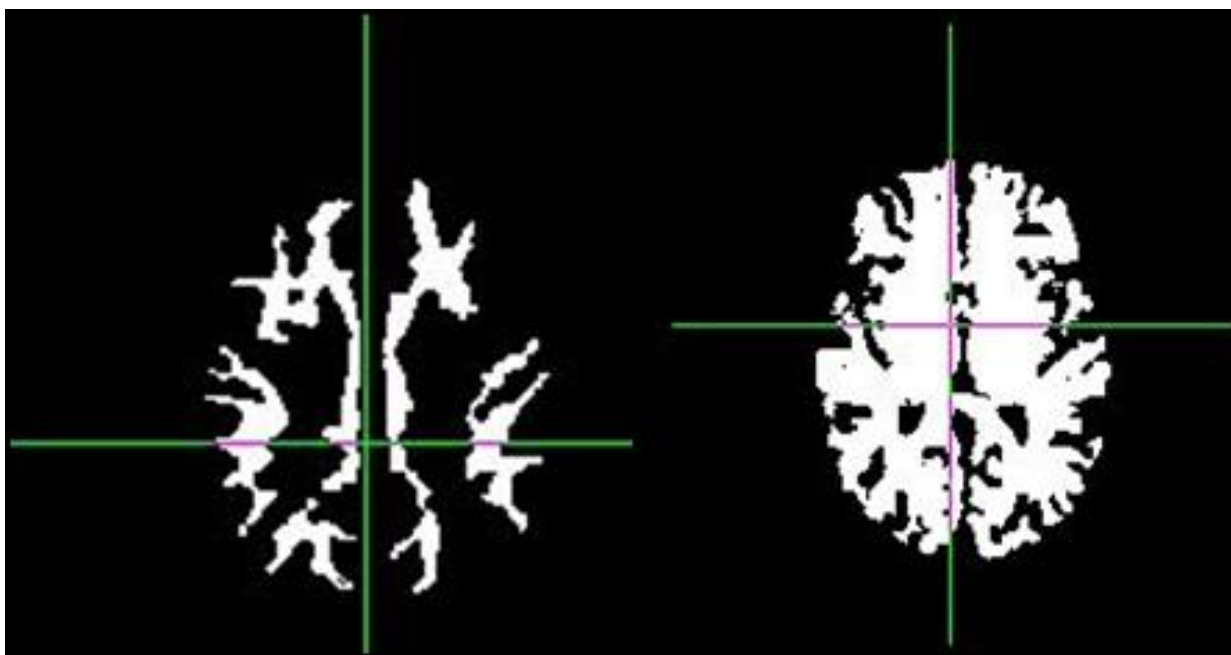
**Figure 2-2 White matter and whole brain segmentation**

White matter (left) and whole brain (right) masks extracted from scan 1 (time point Month -3) of subject P02 using FMRIB's Automated Segmentation Tool.

### 2.4.2.1.  *White Matter and Whole Brain*

The extra-cerebral tissue was removed using BET version 2.1 in FSL (Brain Extraction Tool, FMRIB Software Library, www.fmrib.ox.ac.uk). Segmented masks were created using scan 1 (time point Month -3) (Figure 2-2). A combination of two $T_1$ images (TI = 150 ms and 400 ms) was used to obtain a valid and conservative WM mask. The TI = 1200 ms data was used to create the whole brain mask. Fractional intensity parameters were set at 0.3 for the 150 ms, 0.15 for the 400 ms images and 0.5 for the 1200 ms images. The data was segmented into WM, GM, lesions and CSF using FAST version 4.1 (FMRIB's Automated Segmentation Tool, FMRIB Software Library, www.fmrib.ox.ac.uk). The segmented images were loaded into MATLAB (The Mathworks, MA, USA). The WM segmentation masks of the 150 ms and 400 ms echoes were combined using MATLAB.

In-house software was used to erode the WM and GM masks by 1 voxel in order to minimize potential partial volume error and create a more conservative mask. Small clusters of unwanted pixels (ex. near the edge of the brain) were removed during this process. The masks were eroded twice, and a pixel connectivity of eight was used. Finally a reconstruct function was used to remove remaining unwanted pixel clusters near the brain edge.

All these steps were completed using MATLAB scripts written by Sandra Meyer and modified by Emilie Mackie.

### 2.4.3.  *$T_1$ Maps*

All the MRI data were reconstructed and parametric maps were produced with in house software. $T_1$ relaxation was fit to a single exponential in order to compute voxel-by-voxel

whole brain $T_1$ maps.

$$S(TI) = S(infinity) *(1-f*exp(-TI/T_1) + exp(-TR/T_1)$$

On the $T_1$ maps the various colours and intensities represent different $T_1$ values. The WM and whole brain masks are combined with the $T_1$ map in MATLAB in order to obtain $T_1$ values for each voxel of the segmented masks. For each subject, the $T_1$ values from the WM and the whole brain were used to create histograms. To maintain consistency the scan 1 (Month -3) WM and whole brain masks were used to create $T_1$ histograms at all the time points (M-3, M0, M3, M6).

### 2.4.4. $T_1$ Histograms

$T_1$ histogram analysis is quantitative, reproducible and gives a global measure of tissue water content.[34] To produce $T_1$ histograms the WM and whole brain masks were first applied to the $T_1$ maps resulting in a numerical $T_1$ value for each voxel of the mask. $T_1$ histograms were constructed by binning and summing the individual voxel $T_1$ values for the whole brain and WM. Graphs were created using EXCEL (Microsoft Office 2007). Histograms were normalized by dividing the number of pixels in each bin by the total pixel count and multiplying by 100 to get a percentage. Six histogram features were extracted from each normalized histogram: mean $T_1$ relaxation time, peak height, peak location, and $T_1$ relaxation time value of the 25th, 50th and 75th percentiles.

## 2.5.    *Statistical Analysis*

Values are given as means ± one standard deviation (SD). Statistical analysis was performed using SPSS 2010 for windows package PASW (Predictive Analytics SoftWare). Because of the relatively small number of subjects in the study the differences in $T_1$ histogram features between time points were evaluated using non-parametric statistics. Specifically the Wilcox signed-rank test, a non-parametric statistical hypothesis test for the case of two related samples or repeated measurements on a single sample was used as it can be used as an alternative to a paired Student's t-test when the population cannot be assumed to be normally distributed.

## 3. Results

At present 5 subjects have completed all serial MRI evaluations (subject P07 could not be scanned at month 6 on schedule due to a shoulder injury). For the purpose of this thesis, results from the first 5 subjects are reported (3 females, 2 males, mean age 37 years (range 25-52 years), mean disease duration: 3.6 years (range 1-6 years), median EDSS 2.0). Subjects are labeled by recruitment order (P02, P03, P04, P05, and P07). P01 represented pilot scans of a healthy control and P06 delayed beginning therapy therefore both are excluded from the data presented in this thesis.

### 3.1.  Whole Brain $T_1$

The averaged whole brain $T_1$ histograms in this study exhibit the characteristic profile of data previously recorded for MS patients (Figure 3-3).[81] The highest peak generally occurs at low $T_1$, and represents the WM. The lower, wider peak at higher $T_1$ reflects the more diverse $T_1$ seen in GM.[81] Visually the averaged whole brain $T_1$ histogram profiles changed over time (Figure 3-3). The post treatment $T_1$ profiles moved towards lower $T_1$ values indicating a lowering of water content or an increase in global iron.

### 3.1.1.  Whole Brain $T_1$ Maps: All Subjects

As seen in Figure 3-1 individual subject have different $T_1$ maps. Figure A-1 represents the group mean whole brain $T_1$ histograms across at all time points. We observed that histograms vary widely between different subjects; however the shapes of the histogram profiles remain consistent (for each subject) across all scans. Figure 3-2 shows the evolution of the mean $T_1$

41

values for each subject over all scans. The mean $T_1$ trend-lines vary greatly between subjects. There is no clear pattern that emerges although apart from one outlier the means seem to be decreasing over time in the whole brain.
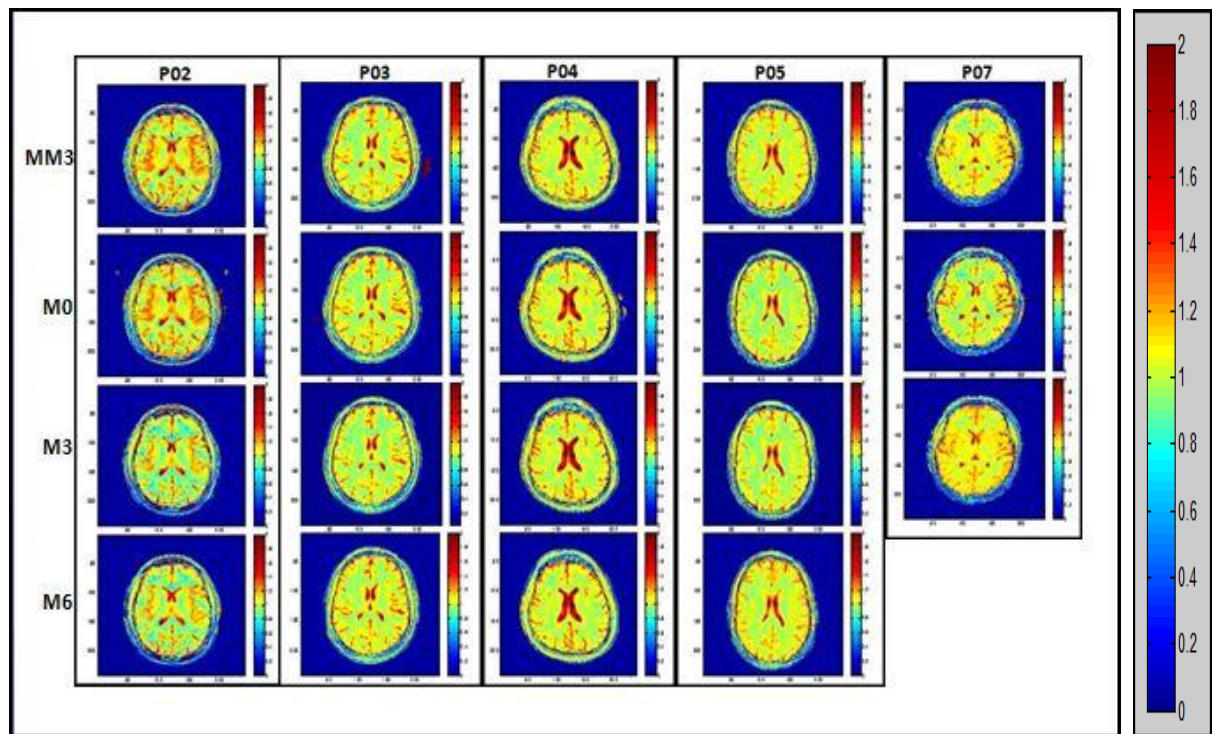
**Figure 3-1 T$_1$ maps**

T$_1$ maps of same slice of all five subjects from all four time points (M-3, M0, M3, M6). In the T$_1$ maps dark red represents a longer T$_1$ time.
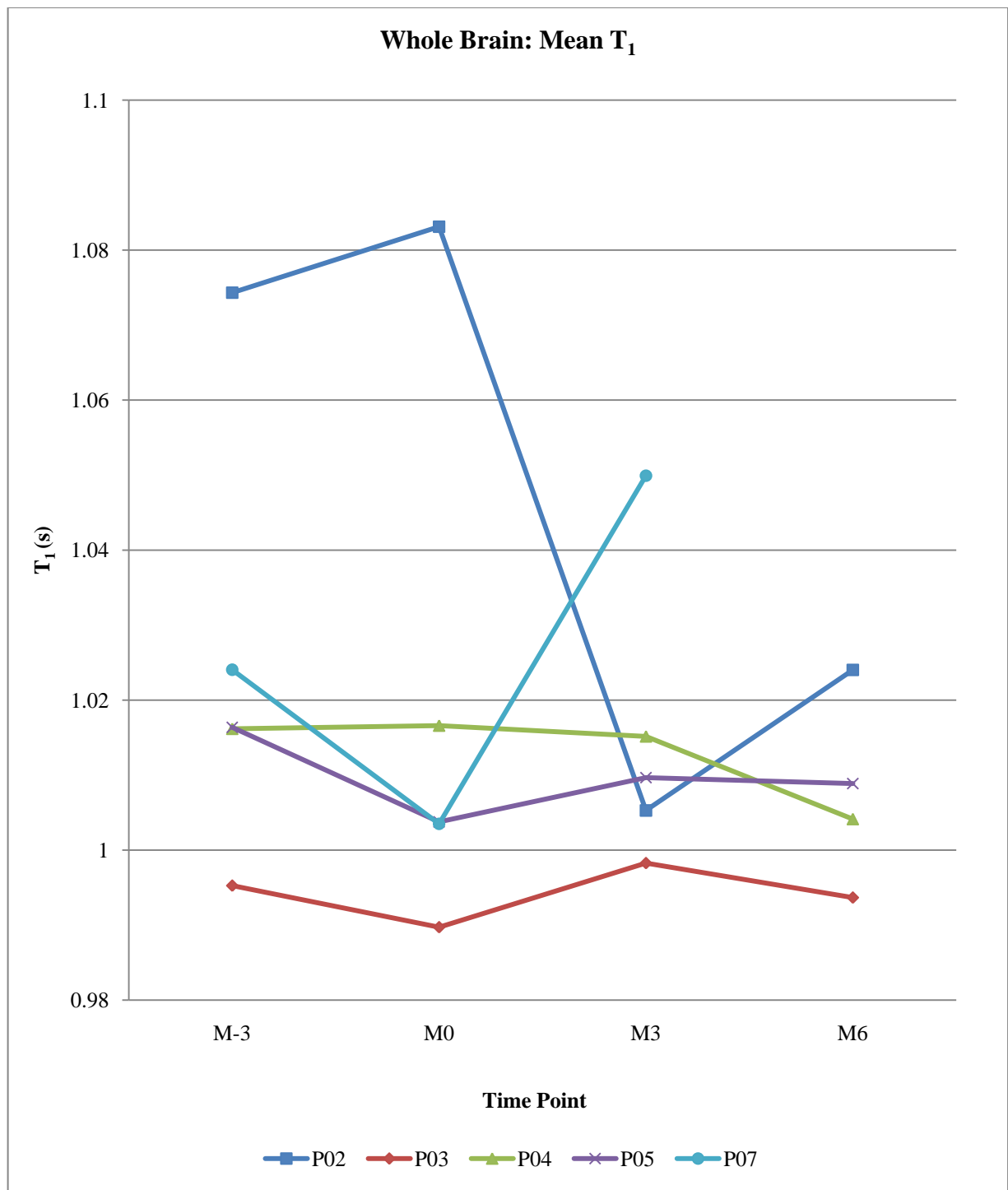
**Figure 3-2 Variation of mean T$_1$ in the whole brain**

Plot of the mean T$_1$ in the whole brain of individual subjects over all four time points (M-3, M0, M3, M6). M-3 and M0 represent the scans prior to initiating DMT; M3 and M6 represent the scans post initation of DMT.

### 3.1.2. *Mean Whole Brain $T_1$ (All Subjects)*

Whole brain histogram metrics were extracted and averaged over all subjects (Figure 3-3). Mean $T_1$ values showed a steady decrease over time (after initiating DMT) from $1.03\pm.03$ s in M-3 to $1.01\pm.01$ s in M6. (Figure 3-4)  This trend is also apparent in the group mean $T_1$ histogram features: peak location, $25^{th}$, $50^{th}$ and $75^{th}$ percentile (Figure 3-4).

Using a Wilcox signed-rank test we compared the group mean $T_1$ histogram features from Month -3 and Month 6. None of the six histogram features were significantly different between Month -3 and Month 6. The mean $T_1$ relaxation time ($p = 0.068$), $25^{th}$ percentile ($p = 0.144$), $50^{th}$ percentile ($p = 0.068$), $75^{th}$ percentile ($p = 0.068$), peak height ($p = 0.465$), peak location ($p = 0.285$).

**Table 3-1 Mean $T_1$ histogram features of the whole brain.** Histogram features were extracted from the $T_1$ histograms using SPSS. Values are means of measured values ± standard deviations.

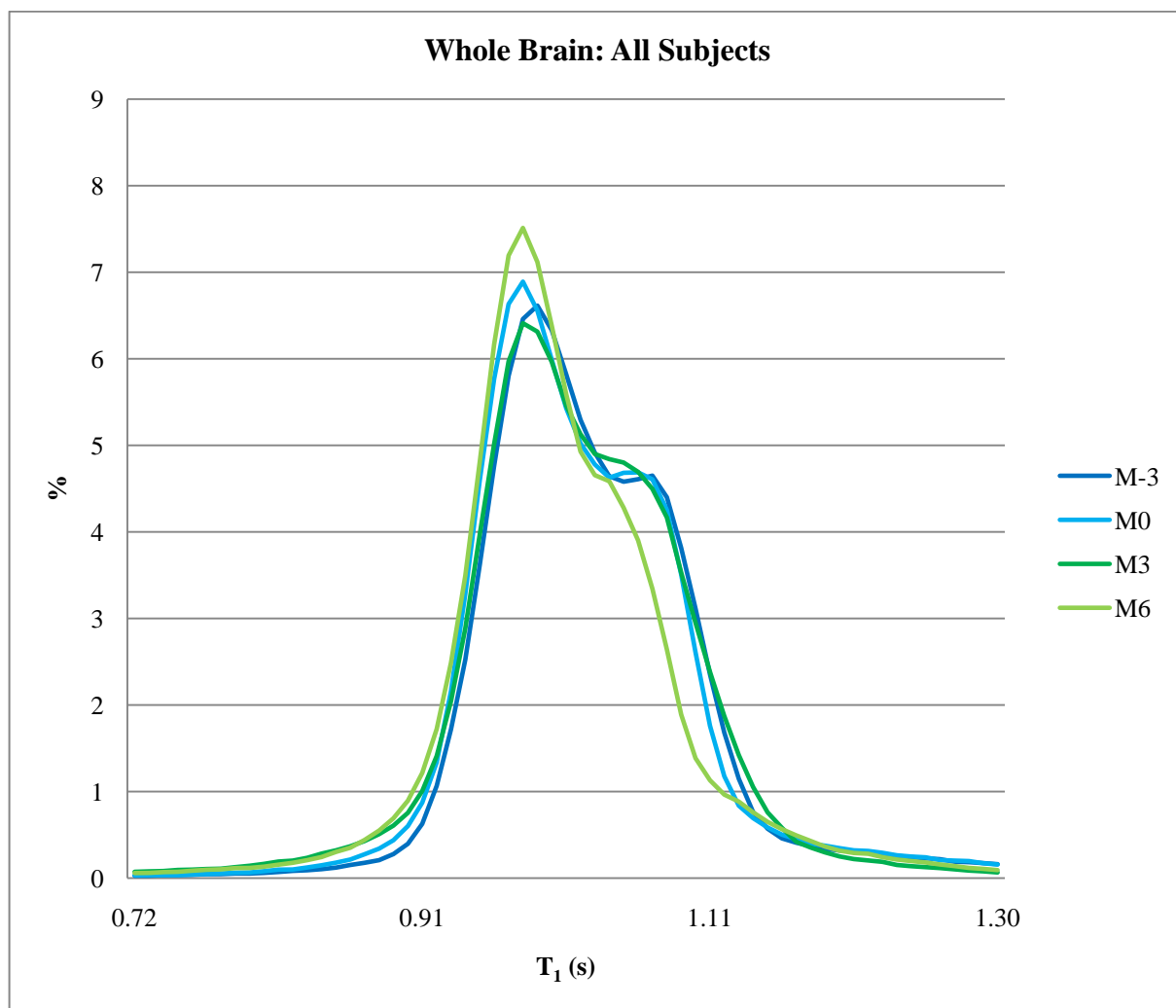| | Whole Brain (All Subjects) | | | |
| --- | --- | --- | --- | --- |
| | Pre-treatment | | During treatment | |
| | M-3 | M0 | M3 | M6 |
| **Mean $T_1$ (s)** | 1.03±0.03 | 1.02±0.04 | 1.02±0.02 | 1.01±0.01 |
| **Max (s)** | 1.36 | 1.42 | 1.42 | 1.50 |
| **25th Percentile (s)** | 0.98±0.01 | 0.97±0.01 | 0.97±0.04 | 0.96±0.02 |
| **50th Percentile (s)** | 1.02±0.02 | 1.01±0.03 | 1.01±0.03 | 1.00±0.00 |
| **75th Percentile (s)** | 1.08±0.05 | 1.07±0.06 | 1.06±0.02 | 1.05±0.03 |
| **Peak Height (%)** | 7.06±2.02 | 7.26±2.32 | 7.3±2.59 | 7.83±2.60 |
| **Peak Location ($T_1$) (s)** | 1.00±0.02 | 0.99±0.02 | 0.99±0.03 | 0.98±0.01 |

**Figure 3-3 Group mean whole brain $T_1$ histograms for each time point**

Normalized whole brain group mean $T_1$ histograms at all four time points. Histograms were normalized by dividing the number of pixels in each bin by the total pixel count and multiplying by 100 to obtain a percentage. Blue lines represent pre DMT scans (M-3 and M0); green lines represent scans after initiating DMT (M3 and M6).
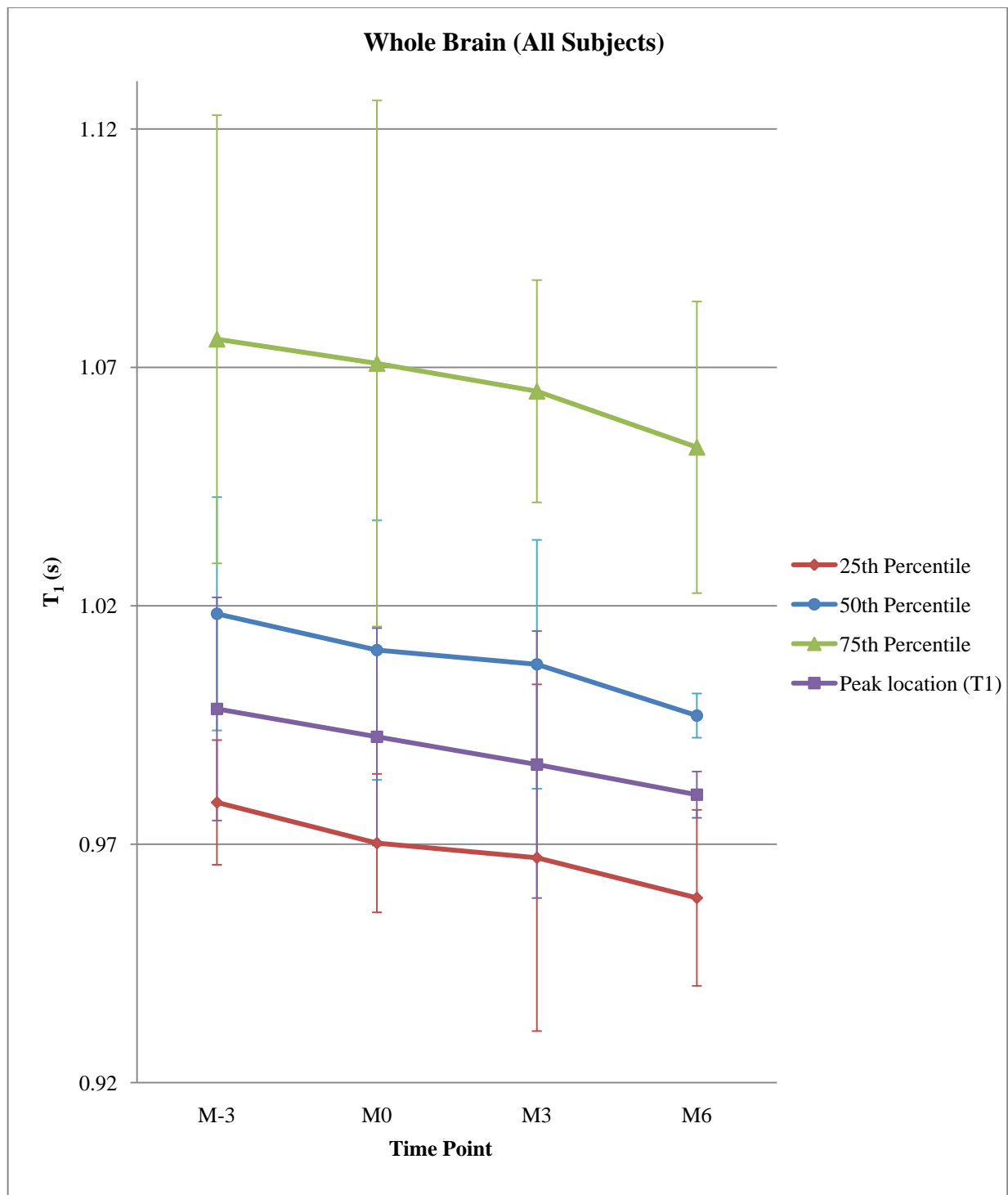
**Figure 3-4 Evolution of whole brain histogram features**

The group mean $T_1$ histogram features: mean $T_1$; peak location (purple), 25th (red), 50th (blue) and 75th (green) percentile of whole brain histograms across all time points.(Error bars represent the standard deviation). All the features show a steady (although not significant) decrease after initiating DMT.
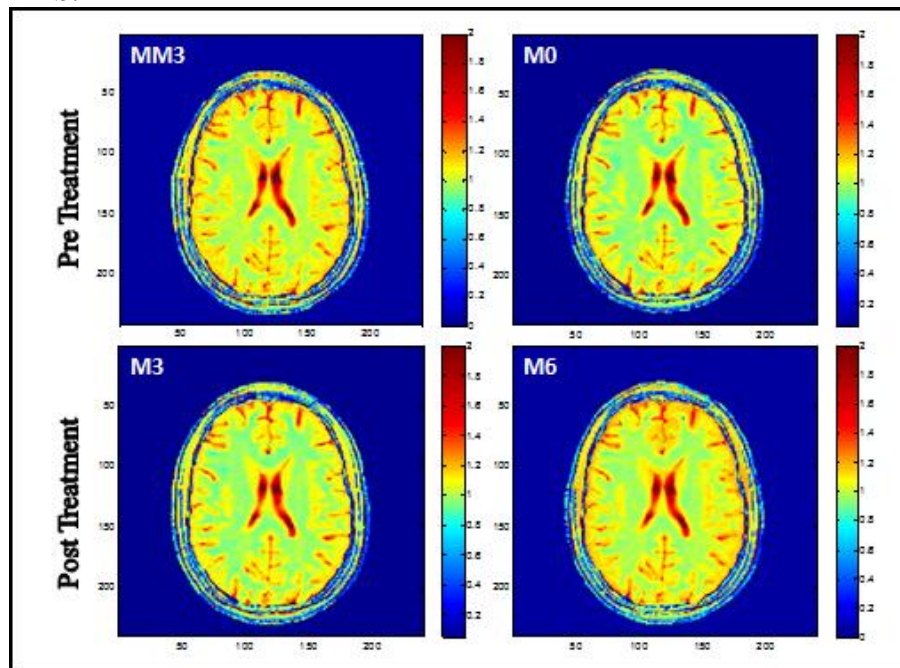
### *3.1.3.    Individual Differences in Whole Brain T$_1$*

Figure 3-5 a. and b. represent the T$_1$ maps for subject P02 and P05 at all time points. The dark red represents a higher T$_1$ signal and therefore higher water content. Visually for subject P02 the T$_1$ maps appear to have higher T$_1$ signals prior to initiating treatment than during the first six months of treatment (this is demonstrated by larger area of yellow and red in pre-treatment maps and more blue in post treatment maps). Subject P05's T$_1$ maps remain similar pre and post-treatment. Figure 3-5 c. and d. are whole brain T$_1$ profiles which represent the normalized T$_1$ histograms. The histogram profiles in Figure 3-5 c. clearly confirm the differences between pre and post-treatment seen in P02's the T$_1$ maps. The whole brain mean T$_1$, peak heights and peak locations M-3 (1.08±0.16 s, 3.96 %, 1.03 s), M0 (1.08±0.16 s, 4.01 %, 1.03 s), M3 (1.01±0.16 s, 3.71 %, 0.95 s) and M6 (1.02±0.16 s, 3.81 %, 0.97 s) indicate a higher T$_1$ signal prior to treatment. Subject P05's T$_1$ histograms (Figure 3-5 d.) are shaped very different from subject P02's. In addition P05 has no noticeable shift between pre and post-treatment histograms. The whole brain mean T$_1$, peak heights and peak locations M-3 (1.02±0.05 s, 9.62%, 0.99 s), M0 (1.00±0.05 s, 9.38 %, 0.98 s), M3 (1.01±0.05 s, 9.13 %, 0.98 s) and M6 (1.01±0.06 s, 9.39 %, 0.98 s) indicate a higher T$_1$ signal prior to treatment.
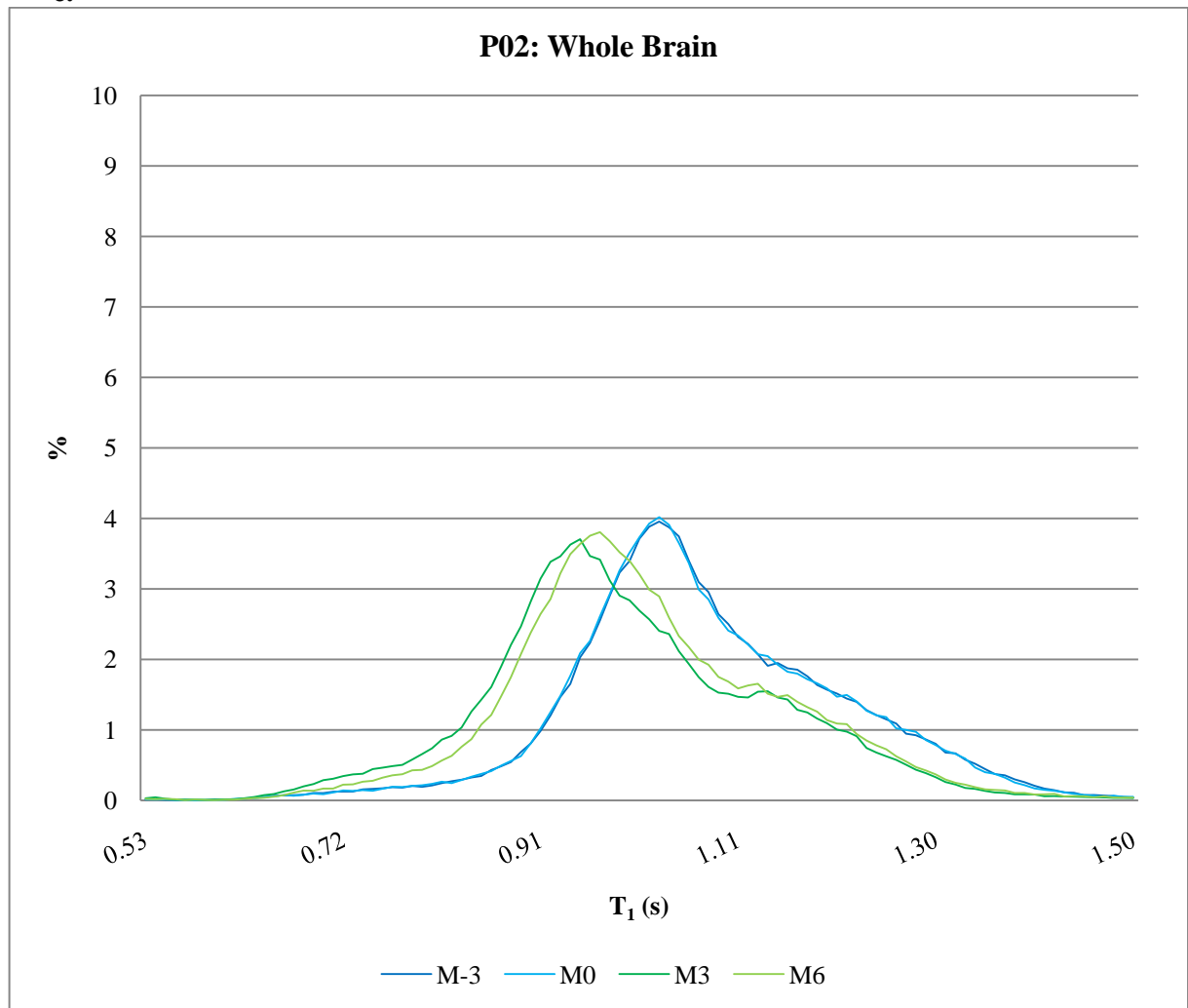
**a.**



**b.**
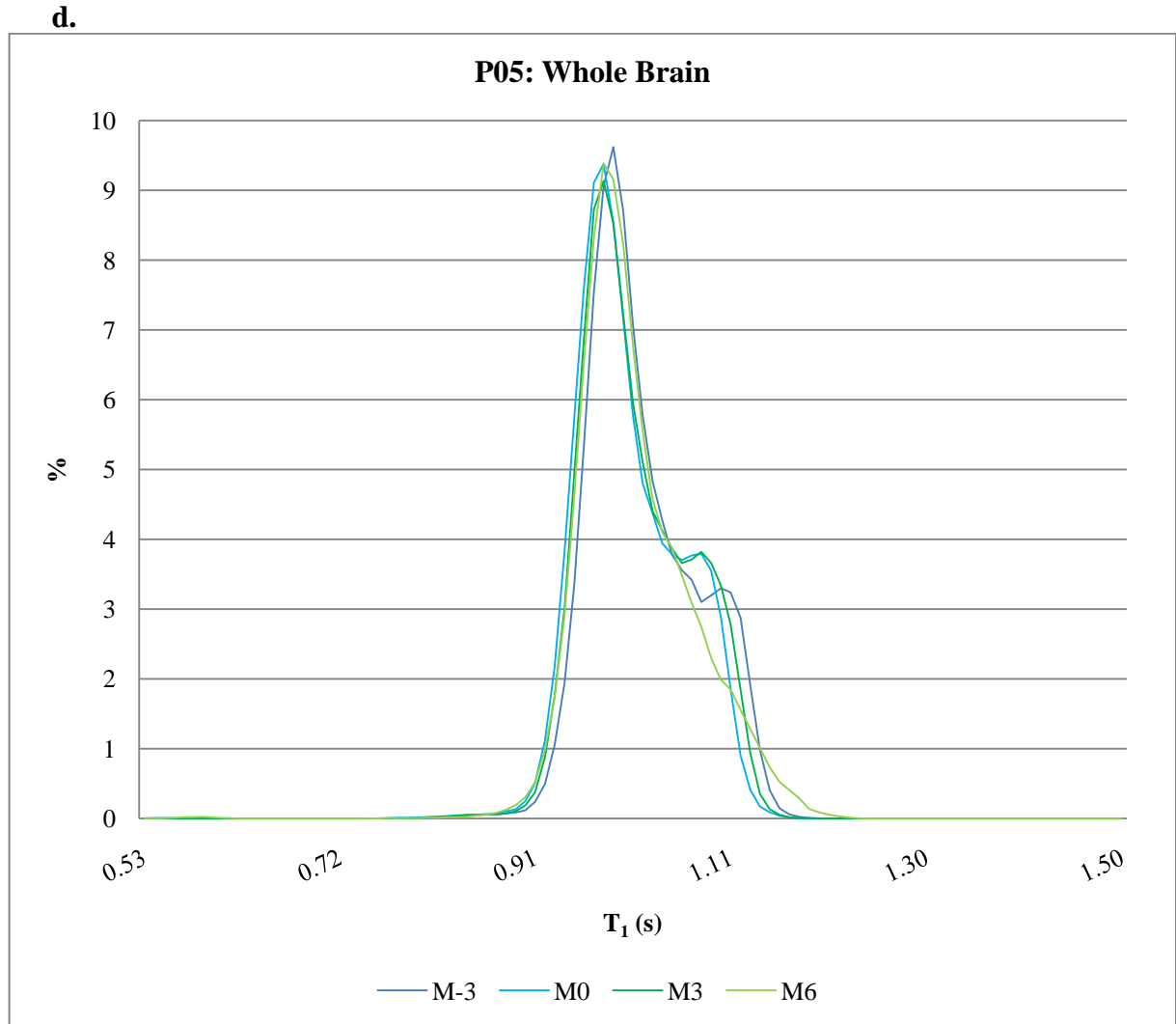
**c.**



P02: Whole Brain

**d.**
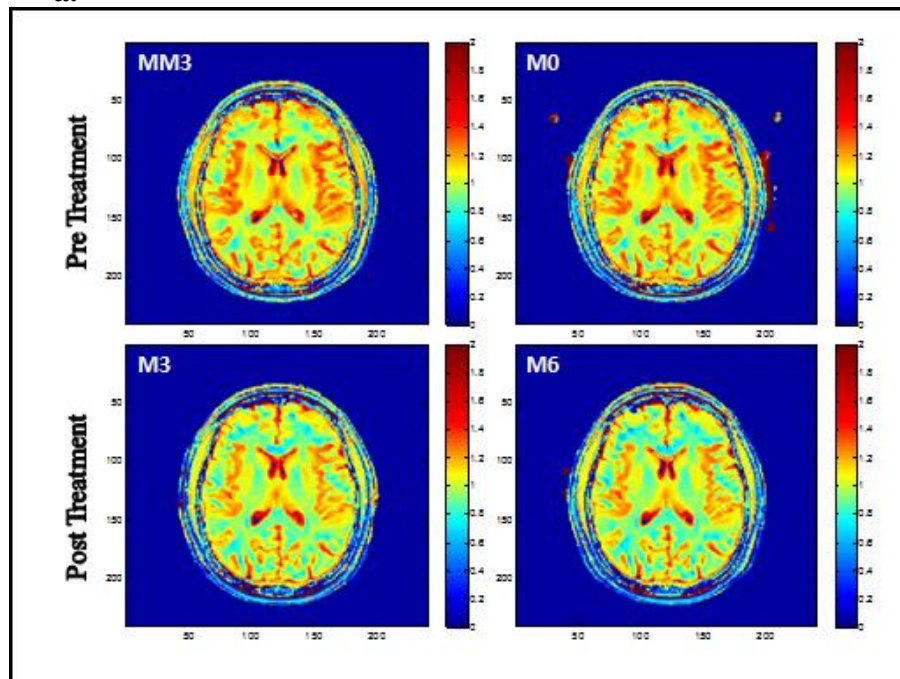


**Figure 3-5 Individual differences in whole brain T$_1$**

All histograms were normalized by dividing the number of pixels in each bin by the total pixel count and multiplying by 100 to obtain a percentage. **(a)** T$_1$ maps for subject P02 at all time points (pre-treatment: M-3, M0; during treatment: M3 and M6) (longer T$_1$ times are indicated by darker red); **(b)** T$_1$ maps for subject P05 at time points M-3, M0, M3 and M6; **(c)** individual normalized whole brain T$_1$ histograms from subject P02 at time points M-3, M0, M3 and M6; **(d)** individual normalized whole brain T$_1$ histograms from subject P05 at time points M-3, M0, M3 and M6 (both horizontal and vertical scales are the same between the two figures). Blue lines represent pre DMT scans (M-3 and M0), green lines represent scans after initiating DMT (M3 and M6). Subject P02's histograms indicate a clear difference in T$_1$ between pre and during treatment scans. However subject P05 does not show the same clear shift in T$_1$.

## 3.2.    *White Matter T$_1$*

As in the whole brain the T$_1$ WM histograms also exhibit the characteristic profile seen in previous studies of MS patients.[81] Visually the group mean WM T$_1$ histogram profiles peaks lowered over time (Figure A-1).

### 3.2.1.    *WM T$_1$: All Subjects*

In WM the mean T$_1$ trend-lines vary greatly between subjects and unlike the whole brain, there is no clear pattern that emerges (Figure 3-6)**.**
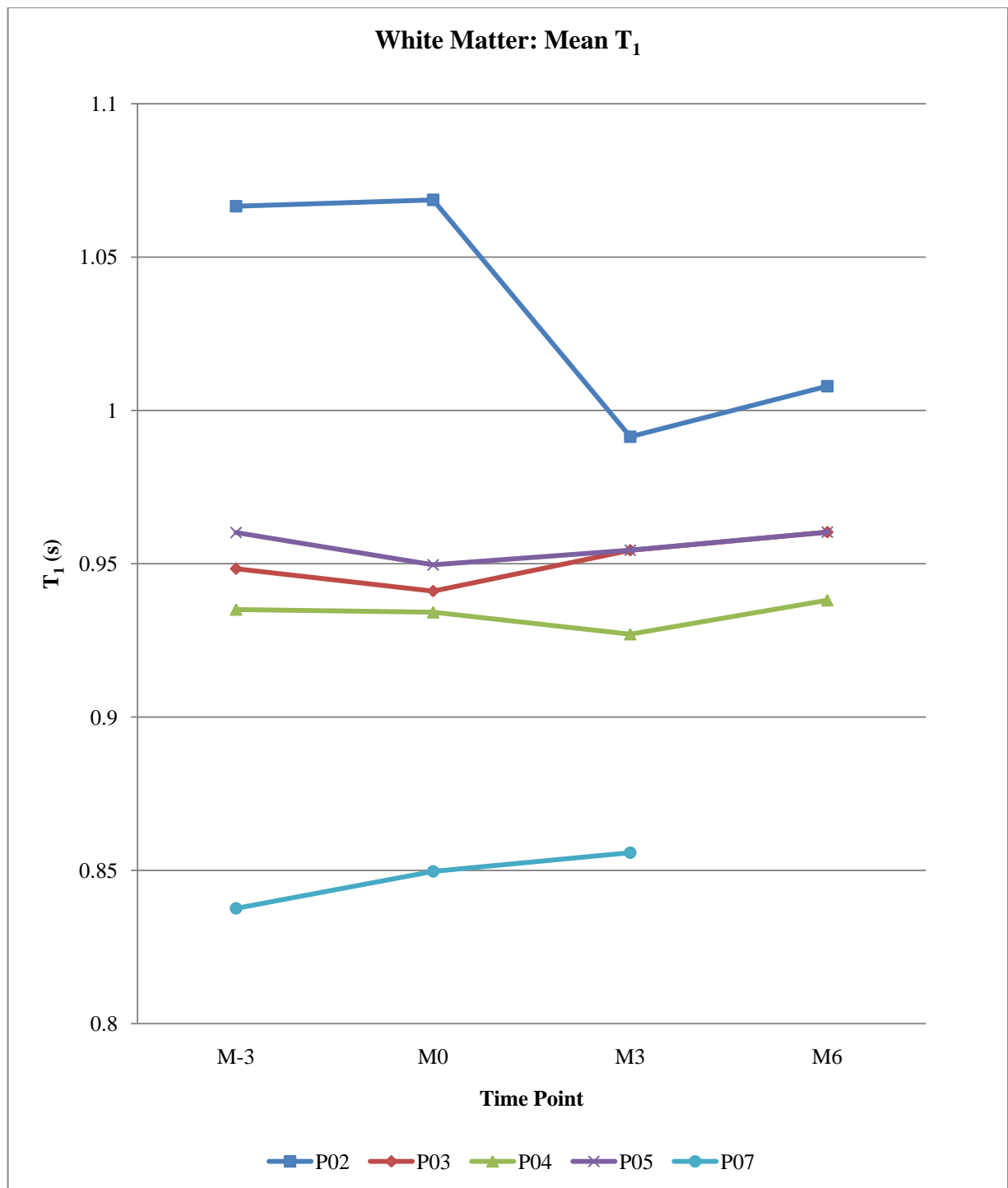
**Figure 3-6 Variation of mean $T_1$ in the white matter**

Plot of the variantion in mean $T_1$ in the WM of individual subjects over all four time points (M-3, M0, M3, M6). Mean $T_1$ was extracted from the $T_1$ histograms. M-3 and M0 represent the scans prior to initiating DMT, at M3 and M6 all subjects are on DMT.

### 3.2.2.    Mean WM $T_1$ (All Subjects)

The WM histogram features were extracted and averaged over all subjects (Table 3-2). Mean $T_1$ values remained constant over time from 0.95±0.08 s in M-3 to 0.97±0.03 s in M6. Unlike in the whole brain the evolution of the 25th, 50th and 75th percentiles and peak location do not indicate any trend (Figure 3-8). Peak height decreased slightly (p = 0.068), 8.82±5.48 s at M-3 to 8.28±3.81 s at M6 and peak location remained constant from M-3 (0.97±0.03 s) to M6 (0.96±0.01 s). This indicates that the range of $T_1$ values in the WM may be widening after treatment. (Figure 3-8)

Using the Wilcox signed-rank test we compared the group mean WM $T_1$ histogram features from M-3 and M6. None of the six histogram features were significantly different between M-3 and M6. The P values of mean $T_1$ relaxation time (p = 0.715), 25th percentile (p = 0.715), 50th percentile (p = 0.715), 75th percentile (p = 1.0), peak height (%) (p = 0.068), peak location (p = 0.414).

**Table 3-2 Mean T$_1$ histogram features of white matter.** Histogram features were extracted from the T$_1$ histograms using SPSS. Values are means of measured values ± standard deviations.

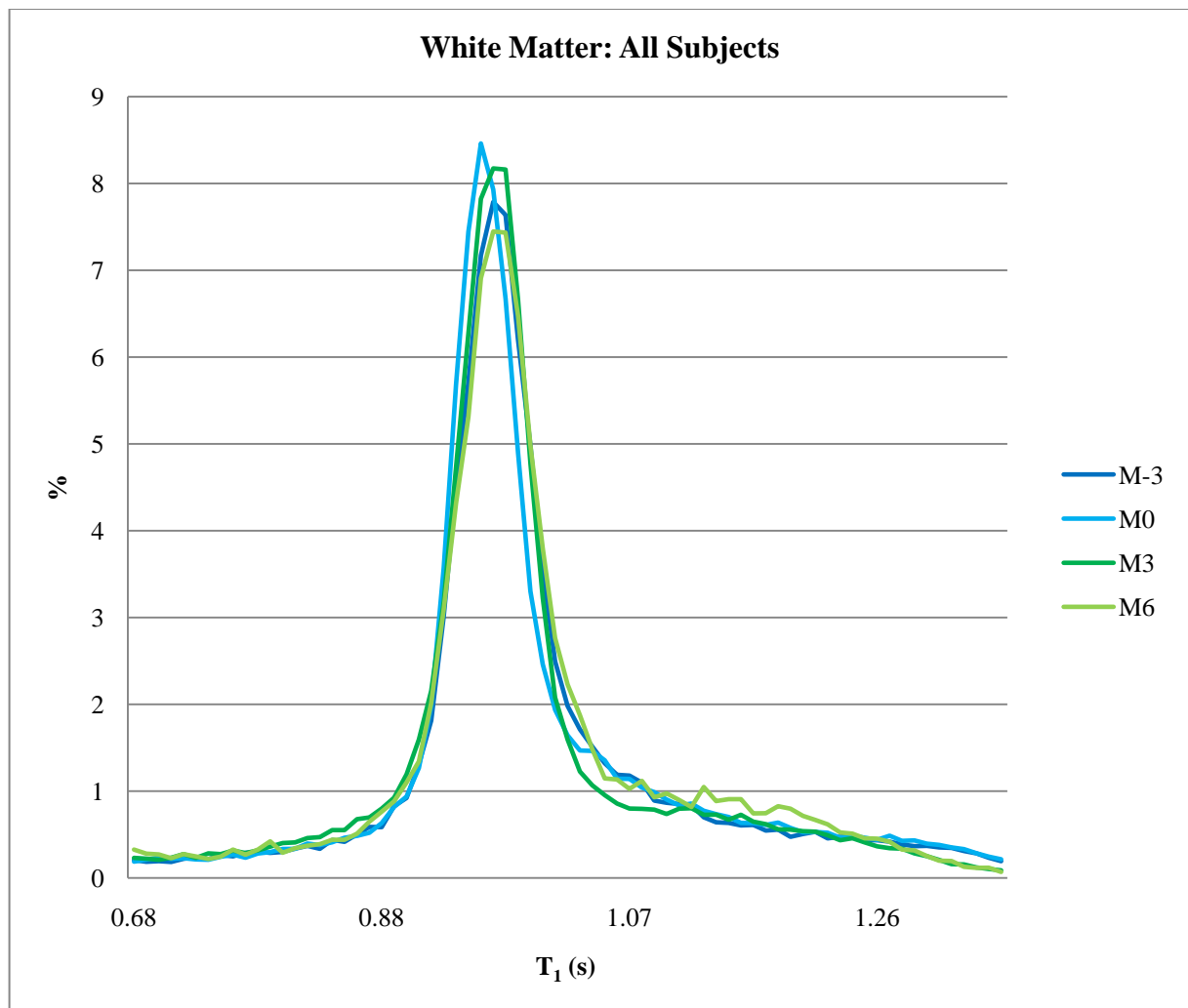| | White Matter (All Subjects) | | | |
|---|---|---|---|---|
| | **Pre-treatment** | | **During treatment** | |
| | **M-3** | **M0** | **M3** | **M6** |
| **Mean T$_1$ (s)** | 0.95±0.08 | 0.95±0.08 | 0.94±0.05 | 0.97±0.03 |
| **Max (s)** | 1.82 | 1.93 | 1.85 | 1.98 |
| **25th Percentile (s)** | 0.88±0.15 | 0.88±0.14 | 0.88±0.11 | 0.94±0.02 |
| **50th Percentile (s)** | 0.97±0.05 | 0.96±0.06 | 0.96±0.01 | 0.97±0.01 |
| **75th Percentile (s)** | 1.04±0.09 | 1.04±0.10 | 1.03±0.06 | 1.03±0.07 |
| **Peak Height (%)** | 8.82±5.48 | 8.93±6.065 | 8.57±5.51 | 8.28±3.81 |
| **Peak Location (T$_1$) (s)** | 0.97±0.03 | 0.98±0.03 | 0.96±0.01 | 0.96±0.01 |

**Figure 3-7 Group mean white matter $T_1$ histograms for each time point**

Normalized group mean WM $T_1$ histograms at all four time points. Histograms were normalized by dividing the number of pixels in each bin by the total pixel count and multiplying by 100 to obtain a percentage. Blue lines represent pre DMT scans (M-3 and M0), green lines represent scans after initiating DMT (M3 and M6).
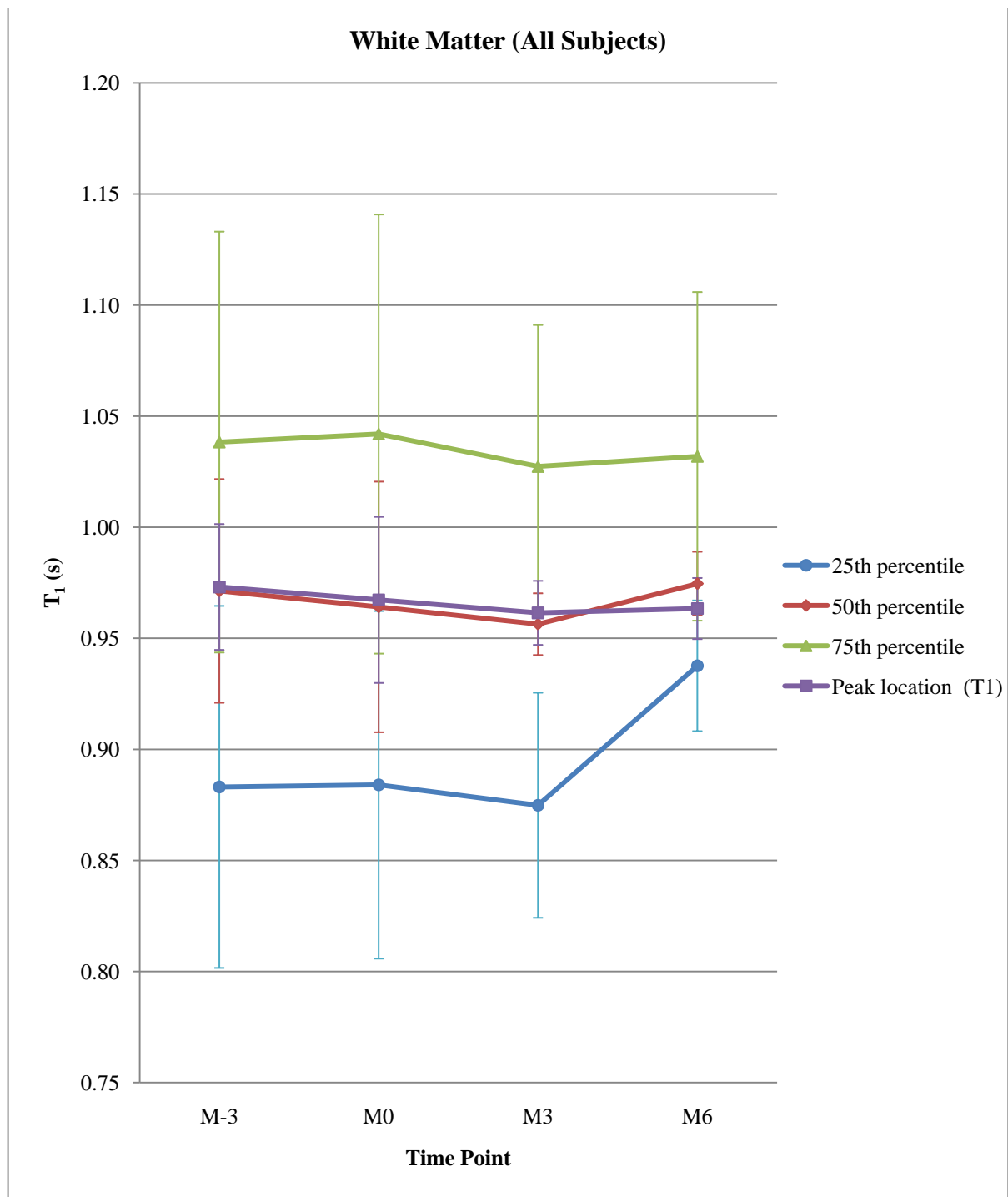
**Figure 3-8 Evolution of white matter histogram features**

The group mean $T_1$ histogram features: $T_1$; peak location (purple), 25th (red), 50th (blue) and 75th (green) percentile of white matter histograms across all time points. (Error bars represent the standard deviation). Unlike in the whole brain the changes 25th, 50th and 75th percentiles and peak location do not indicate any trend

### 3.2.3.    *Individual Differences in WM $T_1$*

Figure 3-9 a. and b. represent the WM $T_1$ profiles of subjects P02 and P05. The observation that histogram profiles of WM are shaped very differently in different subjects is consistent with the whole brain findings.

In subject P02 the WM mean $T_1$, peak heights and locations M-3 (1.07±0.20 s, 3.65 %, 1.02 s), M0 (1.07±0.20 s, 3.59 %, 1.03 s) indicate a higher $T_1$ pre-treatment, M3 (1.00±0.20 s, 3.60 %, 0.94 s) and M6 (1.00±0.20 s, 3.49 %, 0.96 s). This subject started out with a high $T_1$ time before initiating INF beta and returned to where the other subjects were at baseline. In subject P05's histograms there are no shifts in mean $T_1$ or peak location between pre and post treatment however the peak height decreases. Unlike subject P02, the WM mean $T_1$, peak heights and locations of P05 at M-3 (0.96±0.12 s, 15.10 %, 0.97 s), M0 (0.95±0.12 s, 13.31 %, 0.96 s), M3 (0.95±0.12 s, 14.12 %, 0.96 s) and M6 (0.96±0.13 s, 12.27 %, 0.968 s) indicate no difference in $T_1$.

**a.**



P02: White Matter
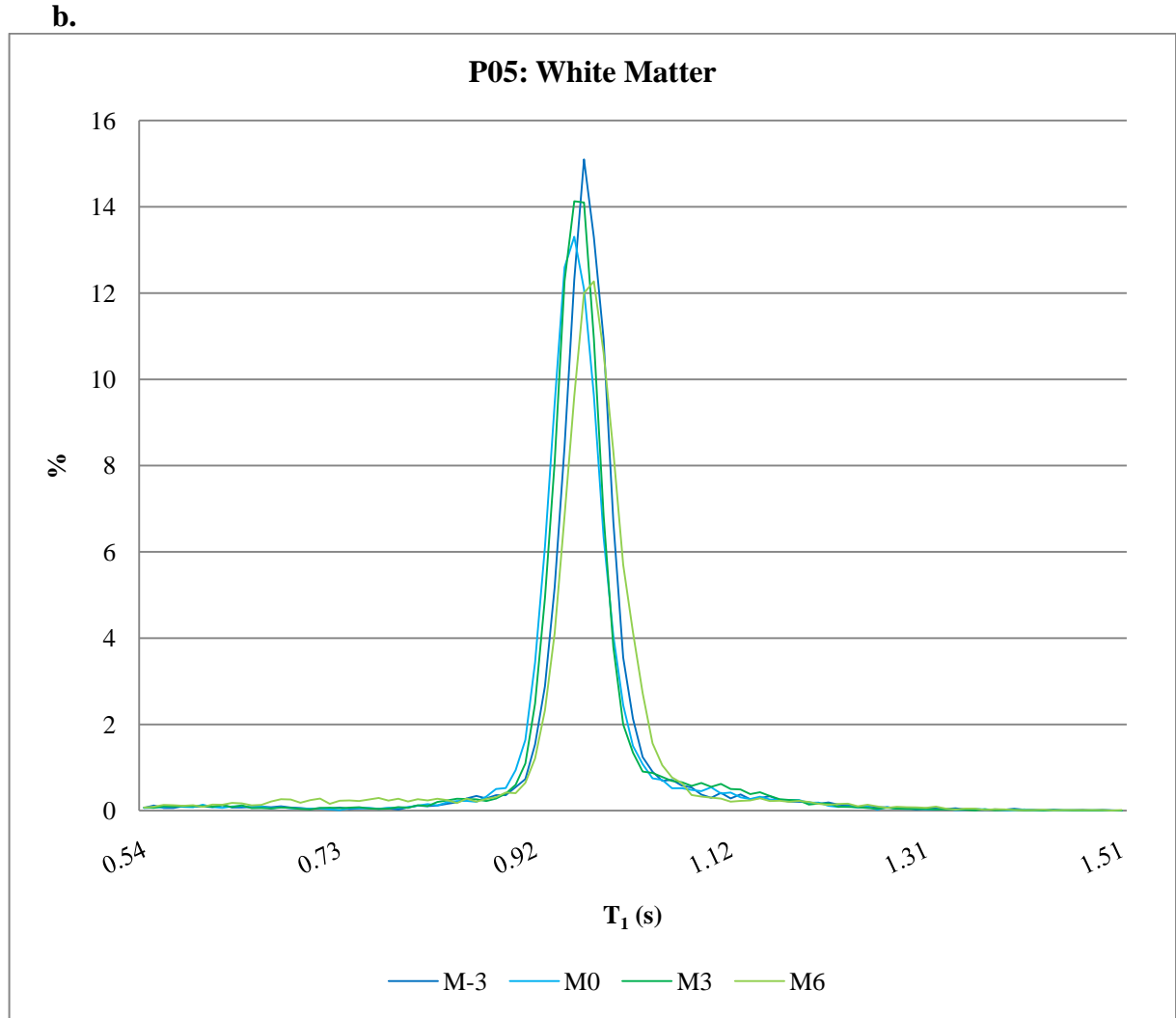
**b.**
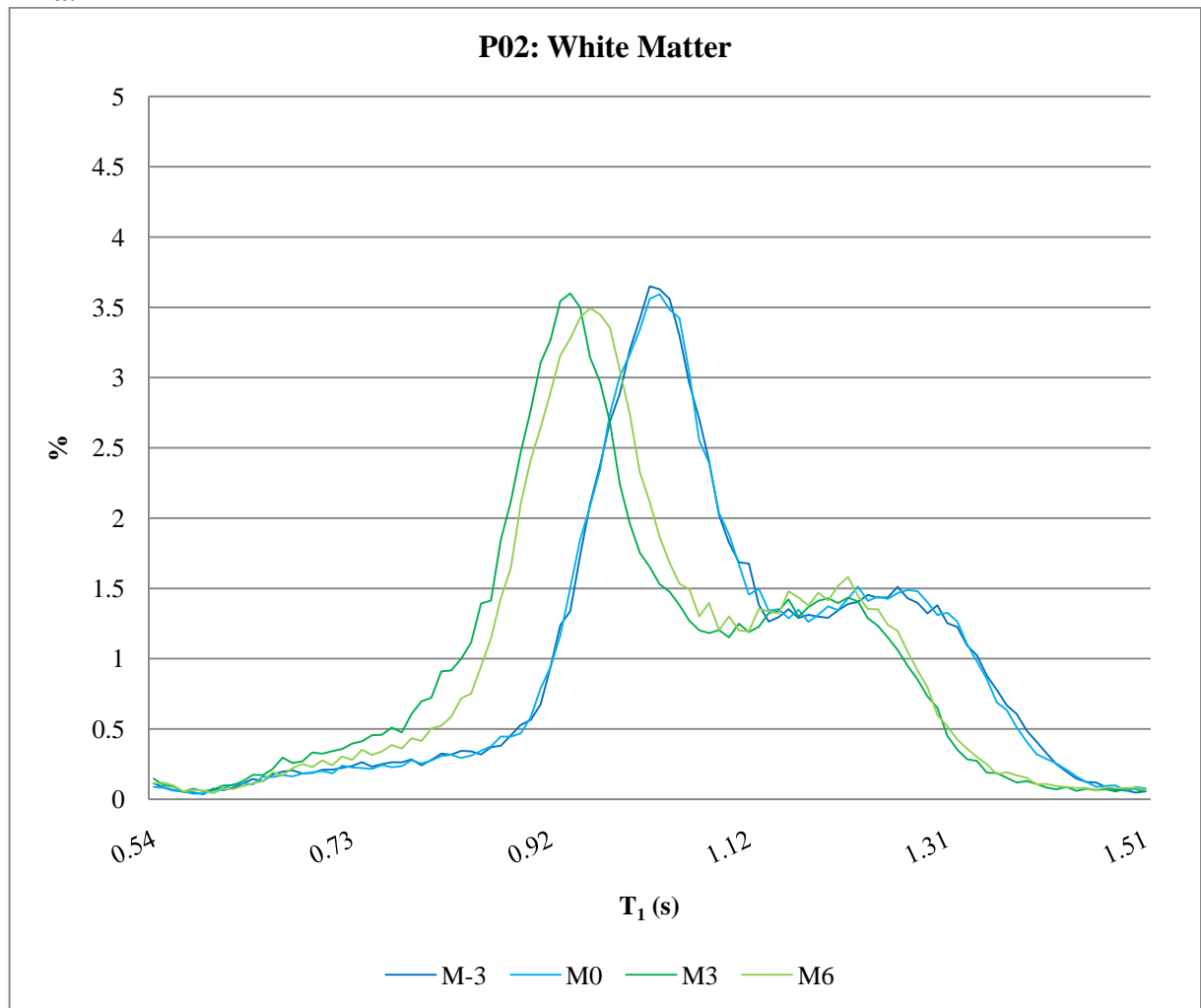


**P05: White Matter**

**Figure 3-9 Individual differences in white matter T$_1$**

Histograms were normalized by dividing the number of pixels in each bin by the total pixel count and multiplying by 100 to obtain a percentage. **(a)** Individual normalized white matter brain T$_1$ histograms from subject P02 at time points M-3, M0, M3 and M6; **(b)** Individual normalized white matter brain T$_1$ histograms from subject P05 at time points M-3, M0, M3 and M6. Blue lines represent pre DMT scans (M-3 and M0), green lines represent scans after initiating DMT (M3 and M6). Subject P02's histograms indicate a clear difference in T$_1$ between pre and during treatment scans. However subject P05 does not show the same clear shift in T$_1$.

## 4. *Discussion*

MRI can be used for sensitive and specific approaches to studying brain water content changes in MS patients initiating DMT. Our hypothesis was that the initiation of INF beta would result in a decrease in brain water content as measured by $T_1$. Although there was no statistically significant decrease in $T_1$ measured in the study population there was a decreasing trend observed in whole brain $T_1$ following the initiation of DMT. This trend was not present in the WM. Different patterns in the shifts of $T_1$ values were seen in different subjects.

## 4.1.    *Comparison of $T_1$ Histograms from the Literature*

$T_1$ measures have been used previously to investigate pathological changes within MS brains. Studies suggest that global measurement of $T_1$ with relaxation times represented as a histogram could provide a good assessment of disease burden.[17, 18, 81-84] Subsequent studies have shown significant differences between MS patients and healthy controls.[84] The $T_1$ histograms of all MS types (RRMS, SPMS, PPMS) show reduced peak heights and shifts towards higher $T_1$ signal values.[83] The $T_1$ measurements in the studies detailed in Table 4-1 were acquired with different MRI protocols at different field strength (1.5 T and 3.0 T). The $T_1$ histograms features measured in this study are in agreement with results previously reported in the literature for the WM and whole brain in MS patients (Table 4-1)**.** In addition $T_1$ histogram profiles are consistent across all studies.

$T_1$ signal increases at higher field strength but is independent of other observation parameters.[83]  At 3.0 T, $T_1$ is expected to be longer, requiring a longer inversion time. As seen in Table 4-1 the present study revealed higher $T_1$ values in both WM and whole brain

compared with previous studies conducted at 1.5 T. $T_1$ values reported in the current study were also similar to the Parry study which is the only study conducted at 3 T.[83]

**Table 4-1** List of studies looking at $T_1$ histogram metrics in the whole brain (WB), WM and GM of MS subjects and healthy controls, at 1.5 and 3.0 T. [17, 18, 81-84]

| Field Strength | Author | WB Peak location (SD) (s) | WB Mean $T_1$ (SD) (s) | WM Peak location (SD) (s) | WM Mean $T_1$ (SD) (s) | GM Peak location (SD) (s) | GM Mean $T_1$ (SD) (s) |
|---|---|---|---|---|---|---|---|
| 1.5T | Griffin et *al.* [81] | **MS** 0.68 (0.11) | **MS** 1.03 (0.07) | - | - | - | - |
| 1.5T | Vrenken et *al.* [82] | - | - | **MS** 0.77 (0.03) | - | **MS** 1.31 (0.06) | - |
| 1.5T | Vaithianathar et *al.* [18] | - | - | 0.61 (0.01) | - | - | - |
| 1.5T | Castriota-Scanderberg et *al.* [84] | - | - | - | **MS** 0.70 (0.03) | - | - |
| 1.5T | Davies et *al.* [17] | - | - | **MS** 0.64 (0.03) **Controls** 0.61 (0.03) | **MS** 0.67 (0.03) **Controls** 0.63 (0.02) | **MS** 1.12 (0.04) **Controls** 1.01 (0.05) | **MS** 1.14 (0.04) **Controls** 1.10 (0.02) |
| 3.0T | Parry et *al.* [83] | - | - | - | **MS** 0.99 (0.09) **Controls** 0.89 (0.02) | - | - |
| 3.0T | Mackie Thesis (2010) | **MS** 1.00 (0.02) | **MS** 1.03 (0.03) | **MS** 0.95 (0.08) | **MS** 0.97 (0.03) | - | - |

Of special interest is the study by Davies et *al.*, which followed 23 patients with early clinically definite RRMS for 26 months (patients were scanned every 6 months).[17] At baseline no patients were taking DMTs, however eight patients began IFN beta during follow up (three prior to 18 month follow-up, two prior to 36 month follow-up). No patients received steroids a month prior to imaging at any time point.[17] Mean $T_1$ and peak location both showed progressive increases in NAWM from baseline (mean: $0.67 \pm 0.03$ s, peak height:

$0.64 \pm 0.03$ s) to 6 month follow-up (mean: $0.68 \pm 0.02$ s, peak height: $0.65 \pm 0.02$ s) although not significant.[17]

## *4.2.* *Variation in Data*

The $T_1$ histogram profiles in this study varied widely between subjects in whole brain and WM (Figure A-1). The most likely explanation for differences between histogram profiles between subjects is natural variations between different brains.[18, 81] Histogram profiles remain consistent for each subject between time points which indicates that the differences are not caused by inconsistencies in the scanner etc. Subjects varied in age, sex, and disease duration and EDSS (3 females, 2 males, mean age 37y (range 25-52y), mean disease duration 3.6 (range 1-6y), mean EDSS 2.0) and these factors may also explain the differences observed.

As mentioned in the previous section the inter-subject differences in the $T_1$ water content shifts that occurred between time points could be the result of inter-subject differences in disease activity, disease burden and BV at baseline (Month -3). Enhancing lesions on an MRI scan indicate active lesions, meaning that there is a breakdown of the BBB and inflammation is present.[6] If a subject (for example subject 2) had a higher level of disease activity (Gadolinium enhancing lesions, DAWM) at Month -3 it could explain the higher $T_1$ at baseline. Studies have shown that $T_1$ values are elevated in lesions and the surrounding tissues.[84] Mean $T_1$ values of black holes (a type of chronic lesion) were significantly higher than mean $T_1$ value of WM in healthy controls and NAWM in MS group.[83] Changes in $T_1$ have been observed in NAWM as well as in lesions, which could contribute, significantly to whole brain and WM $T_1$ values.

### 4.3. Effect of IFN beta on $T_1$ Relaxation Measures of Brain Water Content

Although there were no statistically significant results in this study, the findings in the whole brain $T_1$ over time are very interesting. The lack of significance is likely the result of a lack of statistical power due to the low number of subjects. However this study has provided several interesting and informative observations.

In patients with MS BV is affected by initiating IFN beta. In the first year of phase III clinical trials of IFN beta, researchers found no significant differences or higher decreases in the BV of patients taking IFN beta when compared with placebo groups. However in years two and three there was a substantial reduction in the rate of BV loss in the IFN beta groups.[3]

BV changes in MS involve a combination of volume-gaining and volume-losing processes. Transitory inflammation (edema) and remyelinating processes can cause increases in BV whereas demyelination and neurodegeneration such as axonal loss cause decreases in BV.[3] These changes in BV can be further confounded by anti-inflammatory therapies, which may reduce inflammation, causing the accelerated BV decline called pseudoatrophy which may be caused by decreases in brain water content.

The mechanisms of pseudoatrophy may involve intracellular water being lost due to changes in vascular permeability. It is possible that DMT may lead to irreversible BV loss or true atrophy, possibly due to chemotherapy-induced neuronal toxicity (not shifts in brain water content) but given that BV decrease slows after the first year of treatment this seems

unlikely.[3] At the present we do not understand how DMT prevents or slows BV loss in the long term. It is possible that molecular mechanisms associated with DMTs decelerate BV loss by reducing inflammation and/or promoting repair. However there is no current evidence to support a neuroprotective mechanism or oligodendrocyte (myelin) protection.[3]

Studies examining experimental edema have found that changes in tissue $T_1$ are closely mirrored by changes in tissue hydration.[17] In the current study $T_1$ histograms varied widely between subjects. Disease activity in MS fluctuates and it is likely that reversible or fluctuating pathological processes such as inflammation influence $T_1$ in the brain parenchyma. These factors may explain the inter-subject variation. Different MS subjects may have different amounts of inflammation with differing responses to DMT and hence exhibit differing amounts of pseudoatrophy. This may also explain why the observed changes in $T_1$ fluctuated greatly between time points. Subject P02 had a high $T_1$ before initiating IFN beta, which at M3 and M6 decreased to a $T_1$ similar to that of the other subjects at M-3. Higher $T_1$ time indicates considerable inflammation at baseline while the other subjects had much less inflammation and hence smaller effect on $T_1$ with drug initiation.

Given these results it is possible subjects with longer $T_1$ at M-3 will have a bigger shift at M3. Those with shorter $T_1$ at M-3 may have less inflammation to resolve and therefore have less of a shift. In addition BV changes do not occur at a linear constant rate during pseudoatrophy[3] making it likely that water content changes are also non-linear and therefore more difficult to measure.

Finally the current study did not examine GM because it is very difficult to segment reliably. However given that larger change in whole brain $T_1$ relative to the WM it is possible

that water content in GM may be disproportionately affected by DMT compared to WM.

### 4.3.1.    *Updated Hypothesis*

Analysis of the data indicates that our preliminary hypothesis may be incomplete. Observation of the differences between individuals reveals that different subject's whole brain and WM $T_1$ respond differently to the initiation of DMT. Figure 3-2 and Figure 3-6 represent mean $T_1$ at each time point and illustrates the individual differences graphically. In the whole brain three groups emerged. Group 1, included subject P02; the subject had high $T_1$ signal prior to initiating DMT which decreases to a level comparable with the other subjects after beginning DMT. Subjects in group 2 exhibited minimal change in $T_1$ after initiating DMT. Group 2 includes subjects P03, P04 and P05. Subject P07 represents group 3. Although data from month 6 is missing for this subject, a clear increase in $T_1$ is visible following the initiation of DMT. The] differences observed in the whole brain are also apparent in the WM, with the exception of group 3. In the WM Subject P07's $T_1$ did not increase to the same extent as in the whole brain after initiating DMT.
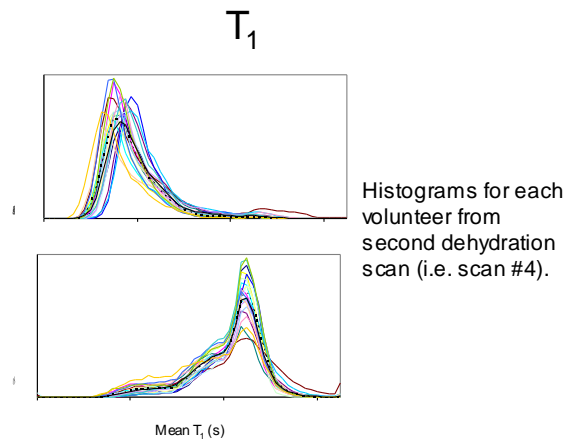
Our hypothesis was that **brain water content (measured by $T_1$) would decrease after initiating DMT**. The results indicate that this hypothesis is incomplete. It is possible that the three groups observed represent different responses to the DMT IFN beta. Group 1 may represent "super responders" to IFN beta or, as mentioned previously, subjects who had a higher level of disease activity (edema) at baseline. Group 2 may represent a group of subjects who don't or minimally respond to IFN beta or subjects who presented with a low level of disease activity (edema). Finally group 3 represents subjects who may become worse after beginning IFN beta.

66

Currently there is not enough data to conclude that subjects will fall into these three groups; however it is an important observation. The observations confirms that it is important to look at the data of individual subjects not simply only as a group.
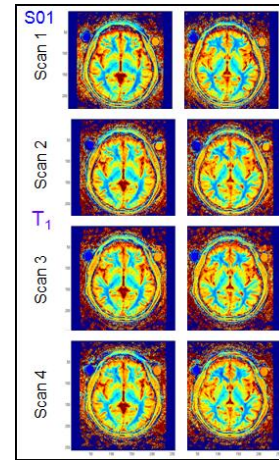
## 4.4. *Reproducibility*

Establishing the reproducibility of our $T_1$ measurements is essential for verifying the validity of this technique. The reproducibility for the $T_1$ technique used in the current study was validated in a previous UBC study. The study involved scanning 20 healthy controls at various levels of hydration over two days.[34] As in the current study histogram profiles varied widely between subjects, in this case healthy controls (Figure 4-1)**.** The $T_1$ measurements were shown to be very reproducible between scans indicating that scanner fluctuations and hydration status did not significantly affect our $T_1$ technique.[34]
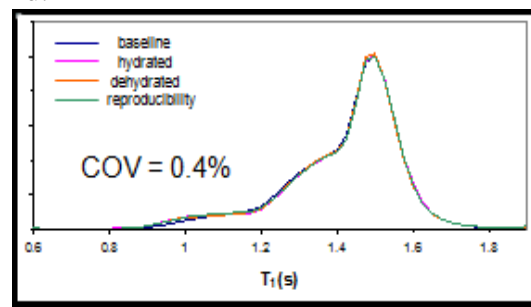
a.

$T_1$

Histograms for each volunteer from second dehydration scan (i.e. scan #4).

Mean $T_1$ (s)

b.

c.

COV = 0.9%

$T_1$(s)

d.

COV = 0.4%

$T_1$(s)
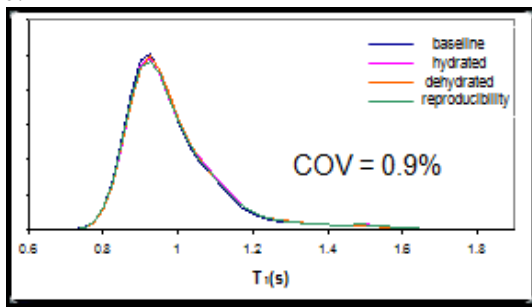
e.

| Tissue | Scan | Histogram Metrics | | |
|---|---|---|---|---|
| | | Mean | peak height | peak location |
| WM | baseline | 0.75 | 6.7% | 0.75 |
| | hydrated | 0.77 | 6.9% | 0.74 |
| | dehydrated | 0.77 | 7.0% | 0.74 |
| | reproducibility | 0.78 | 6.6% | 0.75 |
| GM | baseline | 0.89 | 4.9% | 0.91 |
| | hydrated | 0.88 | 5.8% | 0.91 |
| | dehydrated | 0.88 | 5.4% | 0.91 |
| | reproducibility | 0.89 | 5.2% | 0.92 |

**Figure 4-1 UBC hydration study**

**(a)** Histograms from each volunteer from scan 4 (reproducibility scan) of the UBC hydration study (Top: WM, Bottom: GM); **(b)** $T_1$ maps from one subject in the UBC hydration study (darker red is longer $T_1$); **(c)** $T_1$ histogram profiles of WM in healthy controls in the UBC hydration study (at all four time points: baseline, hydrate, dehydration and reproducibility); **(d)** $T_1$ histogram profiles of GM in healthy controls in the UBC hydration study (at all four time points: baseline, hydrate, dehydration and reproducibility); **(e)** table of histogram metrics from the UBC hydration study [74]

## 4.5.    *Limitations of Study*

The major limitation of this study is the small number of subjects and the lack of data from M6 for subject P07. The goals of this thesis were to establish sound methodology and analyze preliminary data. All statistical analyses have been performed in anticipation of including more subjects. At this point of the study trends are emerging that suggest differences between pre and post-treatment $T_1$ values for whole brain.

In addition this study followed subjects for 7-9 months total (6 months following initiation of DMT); this may not be long enough to observe the full effects of pseudoatrophy.

### 4.5.1.    *$T_1$ as a Measurement of Brain Water Content*

$T_1$ measures of water content have the potential to be a very valuable method for measuring treatment induced changes in brain water content. However there are several limitations in this study. Given the inherent differences between different subjects' histograms the small sample size may result in outliers having a large impact on the results. In addition $T_1$ does not equal brain water content, it is proportional to (*1/(water content) + c (a constant that varies with scanner strength)*) but can be affected by other factors such as iron content.[19, 20] $T_1$ histograms may not be sensitive enough to detect small changes in brain water content. It is also possible that shifts in brain water content caused by pseudoatrophy are compartmental. Therefore measuring changes in whole brain water content may not be representative of regional changes in brain water content.

## 4.6. Ongoing Analysis

As of May $1^{st}$ 2010, 16 subjects have been enrolled in the pseudoatrophy study. In addition to collecting $T_1$ data we are also performing lesion counts to assess disease activity and volumetric analysis.

### 4.6.1. Potential Influence of Disease Activity

As mentioned previously disease activity at the time of the first scan may influence all subsequent $T_1$ measurements. Measuring lesion load at each time point may increase our understanding of how disease activity affects $T_1$. It might also be useful to remove lesions from WM masks to create NAWM masks in addition to the current WM masks

### 4.6.2. MS/MRI Volumetric Analysis

The next step of the study involves analyzing the serial volumetric data for each subject. The volumetric measurement of absolute BPV in this study will be completed by the MS/MRI research group. PD/$T_2$ scans along with the latest image processing techniques will be used to reduce RF inhomogeneity, remove noise, and automatically generate intradural and CSF masks. These masks will be intersected to extract the intricate CSF boundaries within and surrounding the brain. For MS subjects, the result are combined with the quality-controlled lesion masks obtained from a semi-automatic $T_2$ burden of disease analysis to greatly reduce the inaccuracy of measurement due to misclassifying lesion voxels as CSF, which is a common problem in other BV quantification techniques. The final mask computed by the MS/MRI method accurately represents the region composed predominantly of grey and white

matter. The volume of this region divided by the volume of the intradural space gives the BPV. For additional quality control, each mask will be reviewed by a trained technician using specialized in-house software to correct any large-scale errors found in the automated process. The primary advantage of the MS/MRI method is that it is able to obtain an absolute measurement of the fraction of the intradural space occupied by brain tissue (Figure 4-2)**.**

Comparing the $T_1$ and volumetric data will allow us to determine if volumetric changes vary as widely between subjects as $T_1$. This will help us determine the origin of the variations in our $T_1$ data.
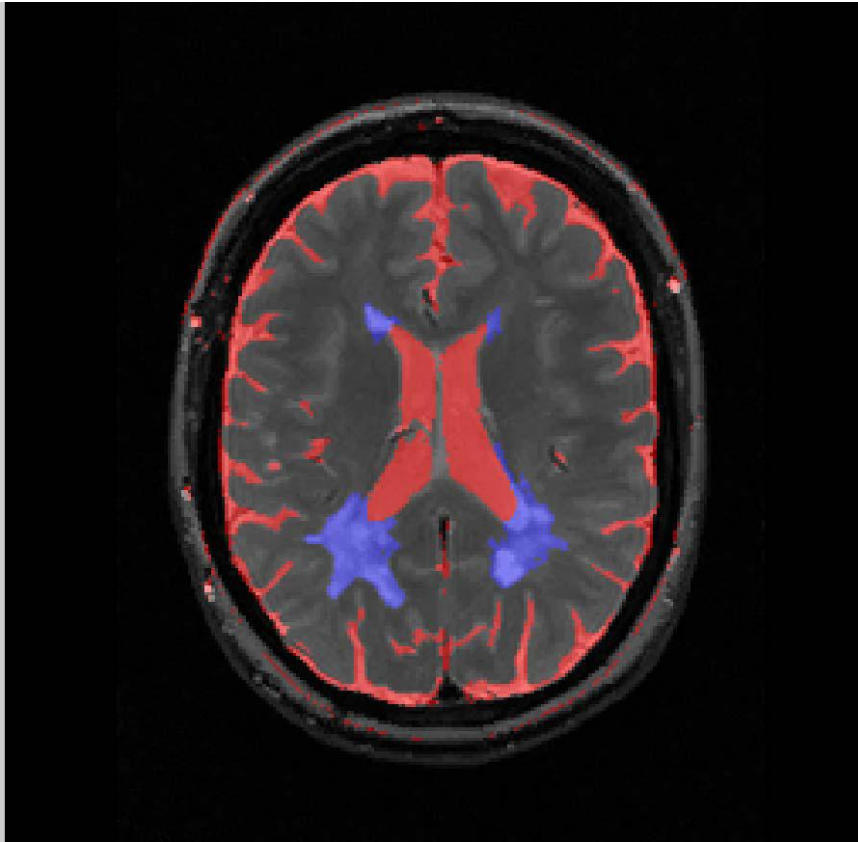
**Figure 4-2 MS/MRI measurement of absolute brain parenchymal volume using PD/T$_2$**

Masks are intersected to extract the intricate CSF boundaries within and surrounding the brain (red). For MS subjects, T$_2$ burden of disease masks (blue) are used to reduce the inaccuracy of measurement due to misclassifying lesion voxels as CSF, which is a common problem in other BV quantification techniques. The final mask computed by our method accurately represents the region composed predominantly of GM and WM. The volume of this region divided by the volume of the intradural space gives the BPV. The primary advantage of the MS/MRI method is that we are able to obtain an absolute measurement of the fraction of the intradural space occupied by brain tissue.

## 5. *Conclusion*

The findings of this study represent the first time that $T_1$ histograms have been used to systematically track changes in water content associated with the initiation of DMT in MS. The results presented in this thesis represent a small number of subjects and continuation of the current methodology is underway; recruiting more subjects to reach an acceptable statistical power level. Upon completion of the study, additional statistical analysis will be required to fully interpret the observations.

Although the statistical power in the current sample size is low the trends apparent in the results suggest several important findings.

$T_1$ histograms measures of the whole brain and WM were compared for changes over time in MS patients before and after they began DMT. MRI's were acquired three months prior to treatment, at baseline, three and six months post treatment. As predicted $T_1$ histograms profiles varied between subjects in both whole brain and WM. It was a consistent finding that the shapes of the histogram profiles remained relatively similar between scans of the same subject acquired during different sessions. The shifts in $T_1$ histograms at different stages of treatment differed greatly between subjects possibly reflecting differences in treatment response from differences in baseline condition as well as individual differences in treatment response.

The averaged $T_1$ histograms of the whole brain and WM were limited by the small number of subjects. In the whole brain comparing the combined mean $T_1$, $25^{th}$, $50^{th}$ and $75^{th}$ percentiles of the $T_1$ histograms at M-3 and M6 demonstrated a trend toward a decrease in $T_1$ ($p = 0.068$) between treated and untreated patients. This suggests that DMT is causing the water content of the whole brain to decrease. In the WM, peak height of the $T_1$ histograms

approached a significant decrease (p = 0.068) and other histogram metrics indicates that $T_1$ histograms are widening.

The $T_1$ measure used in this study offers a non-invasive technique for the assessment of changes in brain water content in-vivo in particular, the changes in brain water content that occur as a result of initiating DMT in MS. This study has established an important methodology that will allow for appropriate interpretations of $T_1$ results in relation to volumetric data. It is probable that future DMT for MS will have anti-inflammatory effects; therefore a better understanding of how therapy affects MR measures of BV is crucial for the development and monitoring of the initiation phase of new treatments. This knowledge will be directly applicable for the development of any new therapeutic modalities using MRI to quantitatively monitor the acute influences on brain water content and potentially disease progression and overall therapeutic efficacy.

# References

1.   Poppe, A.Y., C. Wolfson, and B. Zhu, *Prevalence of multiple sclerosis in Canada: a systematic review.* Can J Neurol Sci, 2008. **35**(5): p. 593-601.
2.   Bakshi, R., *Magnetic resonance imaging advances in multiple sclerosis.* J Neuroimaging, 2005. **15**: p. 5S-9S.
3.   Zivadinov, R., et al., *Mechanisms of action of disease-modifying agents and brain volume changes in multiple sclerosis.* Neurology, 2008. **71**(2): p. 136-44.
4.   Keegan, B.M. and J.H. Noseworthy, *Multiple Sclerosis.* Annual Review of Medicine, 2002. **53**(1): p. 285-302.
5.   Filippi, M., *Multiple sclerosis, Part I: background and conventional MRI. Preface.* Neuroimaging Clin N Am, 2008. **18**(4): p. xv-xvi.
6.   Zivadinov, R. and R. Bakshi, *Role of MRI in multiple sclerosis I: inflammation and lesions.* Front Biosci, 2004. **9**: p. 665-83.
7.   *MR Imaging in White Matter Diseases of the Brain and Spinal Cord.* AJNR Am J Neuroradiol, 2006. **27**(8): p. 1800-1801.
8.   Fatouros, P.P. and A. Marmarou, *Use of magnetic resonance imaging for in vivo measurements of water content in human brain: method and normal values.* J Neurosurg, 1999. **90**(1): p. 109-15.
9.   Zivadinov, R. and R. Bakshi, *Role of MRI in multiple sclerosis II: brain and spinal cord atrophy.* Front Biosci, 2004. **9**: p. 647-64.
10.  Pelletier, D., K. Garrison, and R. Henry, *Measurement of whole-brain atrophy in multiple sclerosis.* J Neuroimaging, 2004. **14**: p. 11S-19S.
11.  Brex, P.A., et al., *Detection of ventricular enlargement in patients at the earliest clinical stage of MS.* Neurology, 2000. **54**(8): p. 1689-91.
12.  Bermel, R.A. and R. Bakshi, *The measurement and clinical relevance of brain atrophy in multiple sclerosis.* Lancet Neurol, 2006. **5**(2): p. 158-70.
13.  Bakshi, R., et al., *Imaging of multiple sclerosis: role in neurotherapeutics.* NeuroRx, 2005. **2**(2): p. 277-303.
14.  Miller, D.H., et al., *Measurement of atrophy in multiple sclerosis: pathological basis, methodological aspects and clinical relevance.* Brain, 2002. **125**(Pt 8): p. 1676-95.
15.  De Stefano, N., M. Battaglini, and S.M. Smith, *Measuring brain atrophy in multiple sclerosis.* J Neuroimaging, 2007. **17**: p. 10S-15S.
16.  Hardmeier, M., et al., *Atrophy is detectable within a 3-month period in untreated patients with active relapsing remitting multiple sclerosis.* Arch Neurol, 2003. **60**(12): p. 1736-9.
17.  Davies, G.R., et al., *Normal-appearing grey and white matter T1 abnormality in early relapsing-remitting multiple sclerosis: a longitudinal study.* Mult Scler, 2007. **13**(2): p. 169-77.
18.  Vaithianathar, L., et al., *White matter T(1) relaxation time histograms and cerebral atrophy in multiple sclerosis.* J Neurol Sci, 2002. **197**(1-2): p. 45-50.
19.  Fatouros, P.P., et al., *In vivo brain water determination by T1 measurements: effect of total water content, hydration fraction, and field strength.* Magn Reson Med, 1991. **17**(2): p. 402-13.

20.     Gelman, N., et al., *Interregional variation of longitudinal relaxation rates in human brain at 3.0 T: relation to estimated iron and water contents.* Magn Reson Med, 2001. **45**(1): p. 71-9.

21.     Kandel, E.R., J.H. Schwartz, and T.M. Jessell, *Principles of neural science.* 4th ed. 2000, New York: McGraw-Hill, Health Professions Division. xli, 1414 p.

22.     Wolthuis, R., et al., *Determination of Water Concentration in Brain Tissue by Raman Spectroscopy.* Analytical Chemistry, 2001. **73**(16): p. 3915-3920.

23.     Segal, M., *Fluid Compartments of the Central Nervous System*, in *The Blood-Cerebrospinal Fluid Barrier.* 2010, CRC Press.

24.     Duning, T., et al., *Dehydration confounds the assessment of brain atrophy.* Neurology, 2005. **64**(3): p. 548-50.

25.     Vander, A.J., J.H. Sherman, and D.S. Luciano, *Human physiology : the mechanisms of body function.* 8th ed. 2001, Boston ; London: McGraw-Hill. xxviii, 800 p.

26.     Shirreffs, S.M., *Markers of hydration status.* Eur J Clin Nutr, 2003. **57 Suppl 2**: p. S6-9.

27.     Amiry-Moghaddam, M. and O.P. Ottersen, *The molecular basis of water transport in the brain.* Nat Rev Neurosci, 2003. **4**(12): p. 991-1001.

28.     Raichle, M.E. and R.L. Grubb, Jr., *Regulation of brain water permeability by centrally-released vasopressin.* Brain Res, 1978. **143**(1): p. 191-4.

29.     Woods, R., et al., *A definition of average brain size, shape and orientation.* Neuroimage, 2000. **11**: p. S615-S615.

30.     Ballabh, P., A. Braun, and M. Nedergaard, *The blood-brain barrier: an overview: structure, regulation, and clinical implications.* Neurobiol Dis, 2004. **16**(1): p. 1-13.

31.     Gullans, S.R. and J.G. Verbalis, *Control of brain volume during hyperosmolar and hypoosmolar conditions.* Annu Rev Med, 1993. **44**: p. 289-301.

32.     Sein, P., et al., *Anorexia nervosa and pseudo-atrophy of the brain.* Br J Psychiatry, 1981. **139**: p. 257-8.

33.     Akiyama, H., et al., *Normal human aging: factors contributing to cerebral atrophy.* J Neurol Sci, 1997. **152**(1): p. 39-49.

34.     Vavasour, I., et al., *Hydration Status Does Not Affect Brain Water Content or Myelin Water Fraction in Healthy Volunteers*, in *MR Probes I*, I.S.f.M.R.i. Medicine, Editor. 2009: Honolulu.

35.     Rooney, W.D., et al., *Magnetic field and tissue dependencies of human brain longitudinal 1H2O relaxation in vivo.* Magn Reson Med, 2007. **57**(2): p. 308-18.

36.     McQuaid, S. and J. Kirk, *The blood-brain barrier in multiple sclerosis.* International Congress Series, 2005. **1277**: p. 235-243.

37.     Laule, C., et al., *Water content and myelin water fraction in multiple sclerosis. A T2 relaxation study.* J Neurol, 2004. **251**(3): p. 284-93.

38.     Stamatovic, S.M., et al., *Inflammation and brain edema: new insights into the role of chemokines and their receptors.* Acta Neurochir Suppl, 2006. **96**: p. 444-50.

39.     Simon, J.H., *Brain atrophy in multiple sclerosis: what we know and would like to know.* Mult Scler, 2006. **12**(6): p. 679-87.

40.     Peterson, J.W., et al., *Transected neurites, apoptotic neurons, and reduced inflammation in cortical multiple sclerosis lesions.* Ann Neurol, 2001. **50**(3): p. 389-400.

41. Fox, et al., *Effects of A[beta] immunization (AN1792) on MRI measures of cerebral volume in Alzheimer disease. [Article].* Neurology May, 2005. **64**(9): p. 1563-1572.

42. Giubilei, F., et al., *Quantitative magnetic resonance analysis in vascular dementia.* J Neurol, 1997. **244**(4): p. 246-51.

43. Ramani, A., J.H. Jensen, and J.A. Helpern, *Quantitative MR imaging in Alzheimer disease.* Radiology, 2006. **241**(1): p. 26-44.

44. Paolillo, A., et al., *The relationship between inflammation and atrophy in clinically isolated syndromes suggestive of multiple sclerosis: a monthly MRI study after triple-dose gadolinium-DTPA.* J Neurol, 2004. **251**(4): p. 432-9.

45. Filippi, M., et al., *Interferon beta-1a for brain tissue loss in patients at presentation with syndromes suggestive of multiple sclerosis: a randomised, double-blind, placebo-controlled trial.* Lancet, 2004. **364**(9444): p. 1489-96.

46. Dalton, C.M., et al., *Early development of multiple sclerosis is associated with progressive grey matter atrophy in patients presenting with clinically isolated syndromes.* Brain, 2004. **127**(5): p. 1101-1107.

47. De Stefano, N., et al., *Evidence of early cortical atrophy in MS: Relevance to white matter changes and disability.* Neurology, 2003. **60**(7): p. 1157-1162.

48. Kalkers, N.F., et al., *Longitudinal brain volume measurement in multiple sclerosis: rate of brain atrophy is independent of the disease subtype.* Arch Neurol, 2002. **59**(10): p. 1572-6.

49. Kalkers, N.F., et al., *Longitudinal Brain Volume Measurement in Multiple Sclerosis: Rate of Brain Atrophy Is Independent of the Disease Subtype.* Arch Neurol, 2002. **59**(10): p. 1572-1576.

50. Lycklama à Nijeholt, G.J., *Reduction of brain volume in MS. MRI and pathology findings.* Journal of the Neurological Sciences, 2005. **233**(1-2): p. 199-202.

51. Inglese, M., B. Benedetti, and M. Filippi, *The relation between MRI measures of inflammation and neurodegeneration in multiple sclerosis.* J Neurol Sci, 2005. **233**(1-2): p. 15-9.

52. Sanfilipo, M.P., et al., *Gray and white matter brain atrophy and neuropsychological impairment in multiple sclerosis.* Neurology March, 2006. **66**(5): p. 685-692.

53. Bermel, R.A., et al., *A semiautomated measure of whole-brain atrophy in multiple sclerosis.* J Neurol Sci, 2003. **208**(1-2): p. 57-65.

54. Kidd, D., et al., *Cortical lesions in multiple sclerosis.* Brain, 1999. **122**(1): p. 17-26.

55. Allen, I.V., et al., *Pathological abnormalities in the normal-appearing white matter in multiple sclerosis.* Neurol Sci, 2001. **22**(2): p. 141-4.

56. Keegan, N.J., F.S. Yudkowitz, and C.A. Bodian, *Determination of the reliability of three scoring systems to evaluate children after general anesthesia.* Anaesthesia, 1995. **50**(3): p. 200-2.

57. Dastidar, P., et al., *Volumes of brain atrophy and plaques correlated with neurological disability in secondary progressive multiple sclerosis.* J Neurol Sci, 1999. **165**(1): p. 36-42.

58. Bakshi, R., et al., *Regional brain atrophy is associated with physical disability in multiple sclerosis: semiquantitative magnetic resonance imaging and relationship to clinical findings.* J Neuroimaging, 2001. **11**(2): p. 129-36.

59. Bermel, R.A., et al., *Bicaudate ratio as a magnetic resonance imaging marker of brain atrophy in multiple sclerosis.* Arch Neurol, 2002. **59**(2): p. 275-80.

60. Fisher, E., et al., *Eight-year follow-up study of brain atrophy in patients with MS.* Neurology, 2002. **59**(9): p. 1412-20.

61. Rudick, R.A., et al., *Brain atrophy in relapsing multiple sclerosis: relationship to relapses, EDSS, and treatment with interferon beta-1a.* Mult Scler, 2000. **6**(6): p. 365-72.

62. Kutzelnigg, A., et al., *Cortical demyelination and diffuse white matter injury in multiple sclerosis.* Brain, 2005. **128**(11): p. 2705-12.

63. Kappos, L.M., et al., *Long-term subcutaneous interferon beta-1a therapy in patients with relapsing-remitting MS.* Neurology September, 2006. **67**(6): p. 944-953.

64. Rudick, R.A., et al., *Management of Multiple Sclerosis.* N Engl J Med, 1997. **337**(22): p. 1604-1611.

65. Zivadinov, R., et al., *The place of conventional MRI and newly emerging MRI techniques in monitoring different aspects of treatment outcome.* J Neurol, 2008. **255**: p. 61-74.

66. Rudick, R.A., et al., *Use of the brain parenchymal fraction to measure whole brain atrophy in relapsing-remitting MS. Multiple Sclerosis Collaborative Research Group.* Neurology, 1999. **53**(8): p. 1698-704.

67. Hardmeier, M., et al., *Rate of brain atrophy in relapsing MS decreases during treatment with IFNbeta-1a.* Neurology, 2005. **64**(2): p. 236-40.

68. Molyneux, P.D., et al., *The effect of interferon beta-1b treatment on MRI measures of cerebral atrophy in secondary progressive multiple sclerosis.* Brain, 2000. **123**(11): p. 2256-2263.

69. Rao, A.B., et al., *Methylprednisolone effect on brain volume and enhancing lesions in MS before and during IFNbeta-1b.* Neurology, 2002. **59**(5): p. 688-94.

70. Hoogervorst, E.L., C.H. Polman, and F. Barkhof, *Cerebral volume changes in multiple sclerosis patients treated with high-dose intravenous methylprednisolone.* Multiple Sclerosis, 2002. **8**(5): p. 415-419.

71. Filippi, M.M., et al., *Whole brain volume changes in patients with progressive MS treated with cladribine. [Article].* Neurology December, 2000. **55**(11): p. 1714-1718.

72. Rovaris, M., et al., *Short-term brain volume change in relapsing-remitting multiple sclerosis: Effect of glatiramer acetate and implications.* Brain, 2001. **124**(9): p. 1803-1812.

73. Sormani, M.P., et al., *Measurement error of two different techniques for brain atrophy assessment in multiple sclerosis.* Neurology, 2004. **62**(8): p. 1432-4.

74. Savazzi, G.M., F. Cusmano, and S. Musini, *Cerebral Imaging Changes in Patients with Chronic Renal Failure Treated Conservatively or in Hemodialysis.* Nephron, 2001. **89**(1): p. 31-36.

75. Yamanouchi, H., et al., *Reversible altered consciousness with brain atrophy caused by valproic acid.* Pediatric Neurology, 2003. **28**(5): p. 382-384.

76. Walters, R.J.L., et al., *Haemodialysis and Cerebral Oedema.* Nephron, 2001. **87**(2): p. 143-147.

77. Noseworthy, J.H., *How much can we learn from long-term extension trials in multiple sclerosis?* Neurology, 2006. **67**(6): p. 930-931.

78. Dalton, C., et al., *Effect of natalizumab on conversion of gadolinium enhancing lesions to T1 hypointense lesions in relapsing multiple sclerosis.* Journal of Neurology, 2004. **251**(4): p. 407-413.
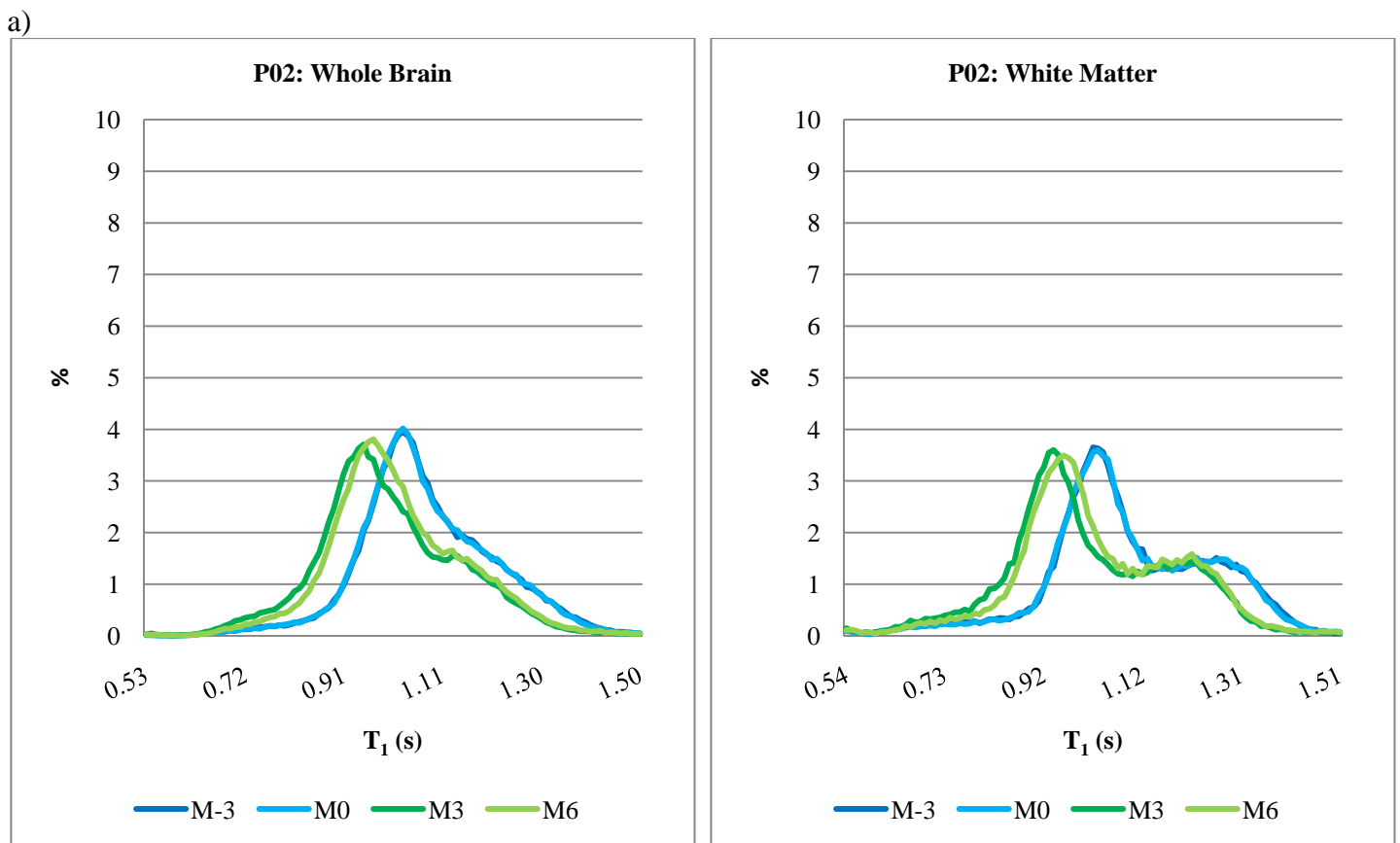
79.    Filippi, M., et al., *Glatiramer acetate reduces the proportion of new MS lesions evolving into "black holes".* Neurology, 2001. **57**(4): p. 731-3.

80.    Simon, J.H., et al., *A longitudinal study of T1 hypointense lesions in relapsing MS: MSCRG trial of interferon beta-1a. Multiple Sclerosis Collaborative Research Group.* Neurology, 2000. **55**(2): p. 185-92.

81.    Griffin, C.M., et al., *T1 histograms of normal-appearing brain tissue are abnormal in early relapsing-remitting multiple sclerosis.* Mult Scler, 2002. **8**(3): p. 211-6.

82.    Vrenken, H., et al., *Whole-brain T1 mapping in multiple sclerosis: global changes of normal-appearing gray and white matter.* Radiology, 2006. **240**(3): p. 811-20.

83.    Parry, A., et al., *White matter and lesion T1 relaxation times increase in parallel and correlate with disability in multiple sclerosis.* J Neurol, 2002. **249**(9): p. 1279-86.

84.    Castriota-Scanderbeg, A., et al., *T1 relaxation maps allow differentiation between pathologic tissue subsets in relapsing-remitting and secondary progressive multiple sclerosis.* Mult Scler, 2004. **10**(5): p. 556-61.

## A. Additional Figures

**Figure A-1 Histogram profiles (All Subjects)**

The normalized whole brain and white matter $T_1$ histogram profiles for each subject at each time point. Histograms were normalized by dividing the number of pixels in each bin by the total pixel count and multiplying by 100 to obtain a percentage. This figure illustrates the inter-subject differences in histogram profiles and the consistency of subject's histogram profiles at all time points. Vertical scales differ between some of the figures **(a)** P02; **(b)** P03; **(c)** P04; **(d)** P05; **(e)** P07

a)

b)



c)

d)

**P05: Whole Brain**



**P05: White Matter**
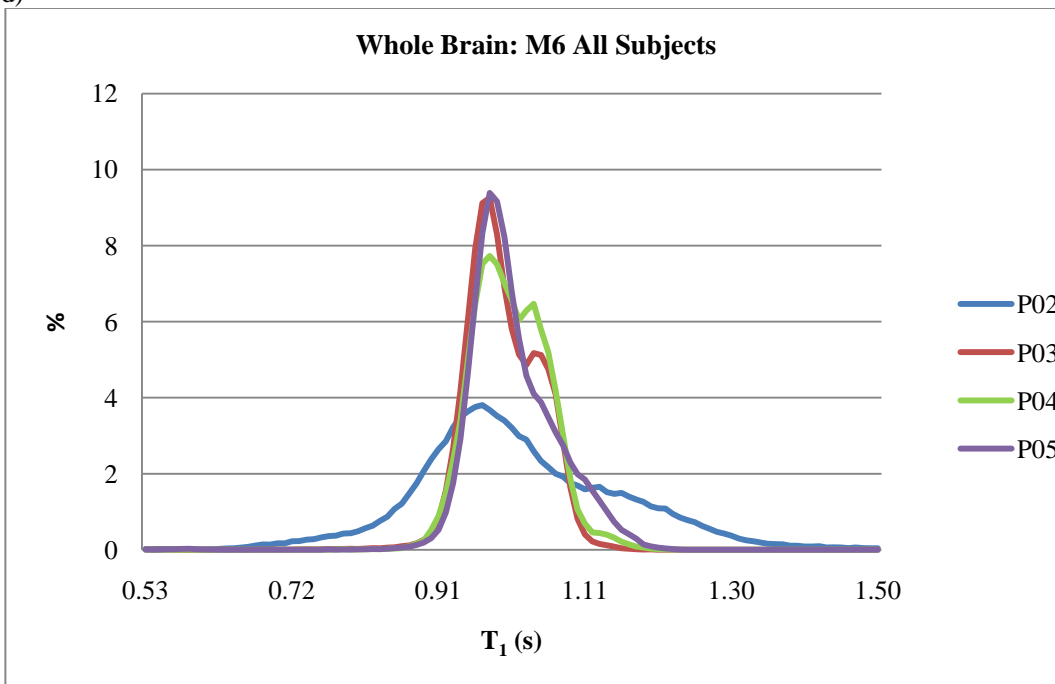


e)

**P07: Whole Brain**



**P07: White Matter**
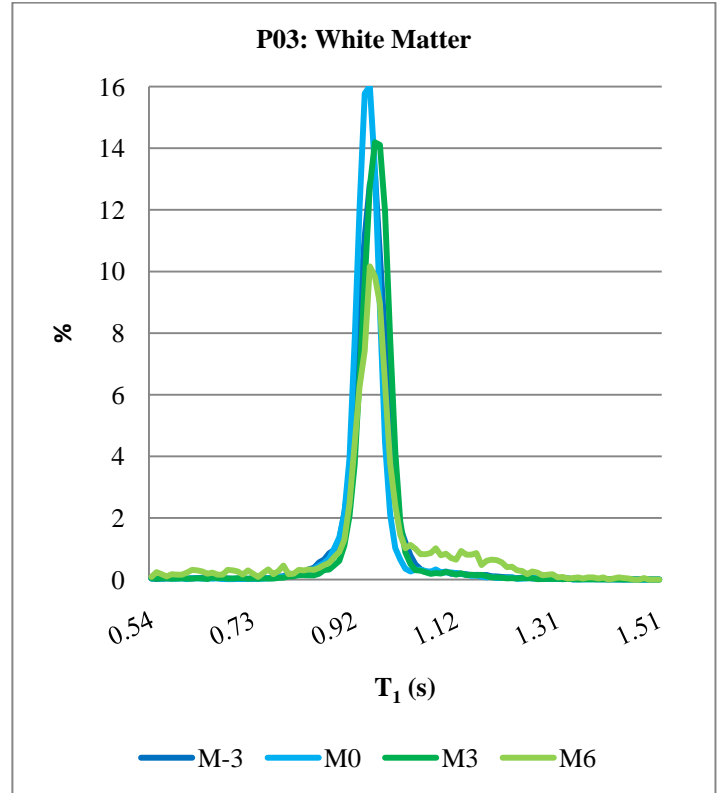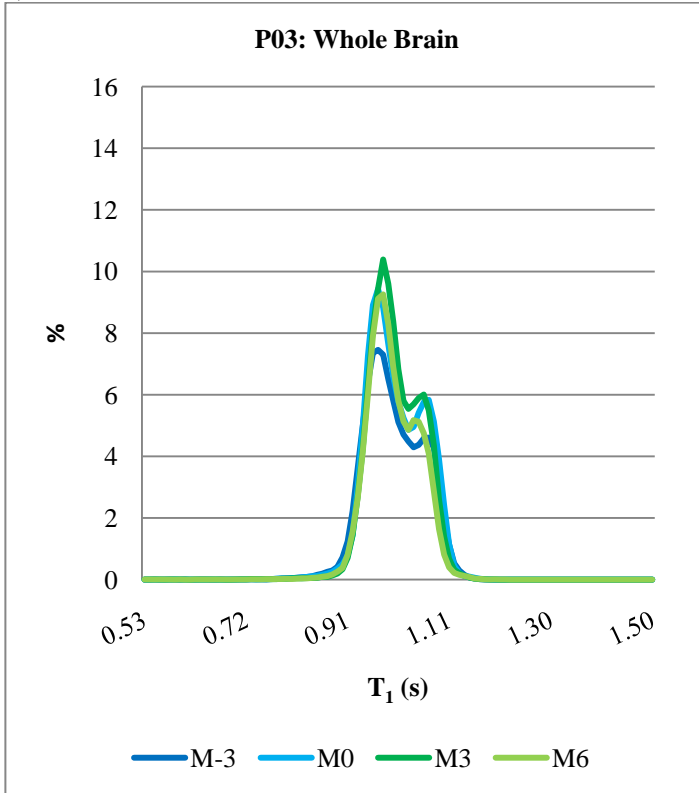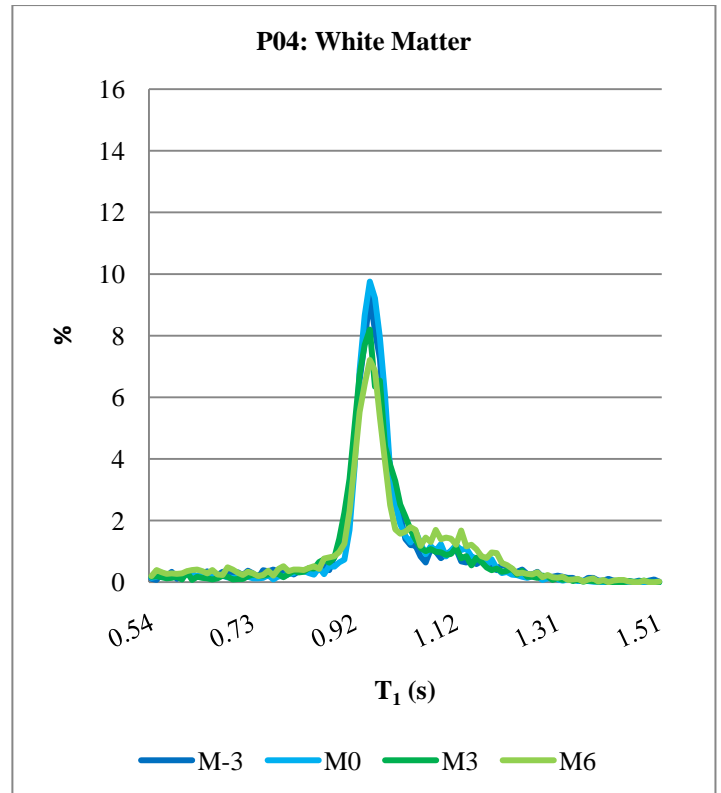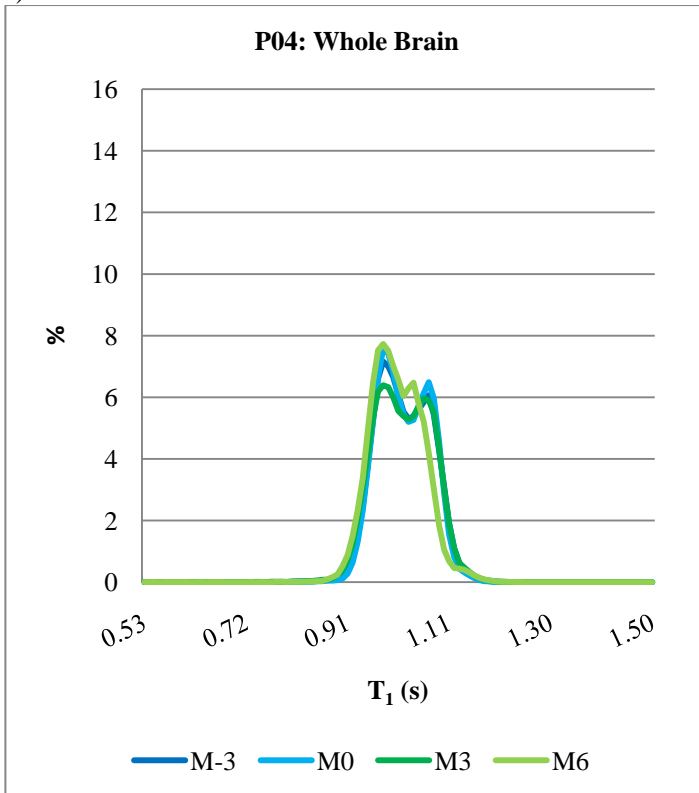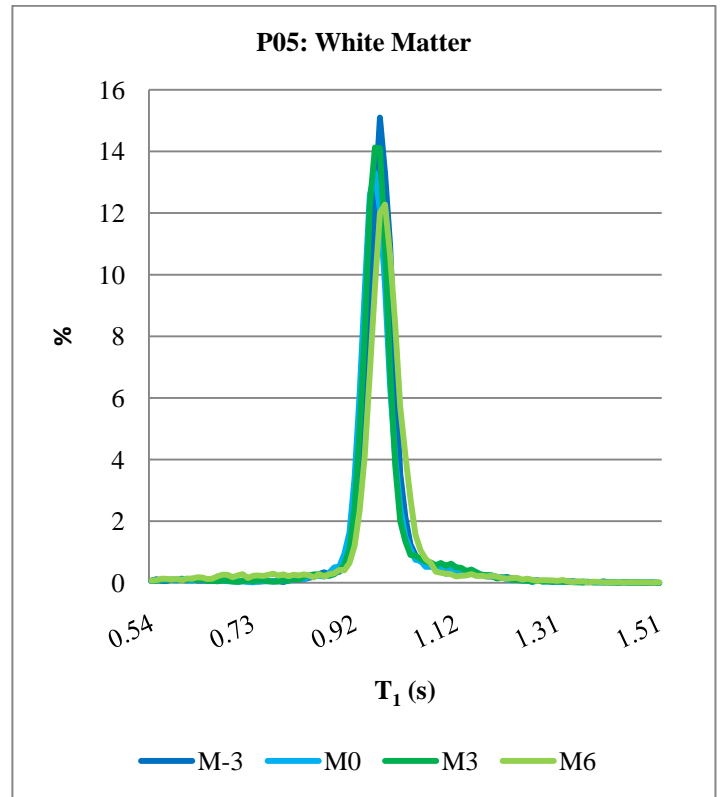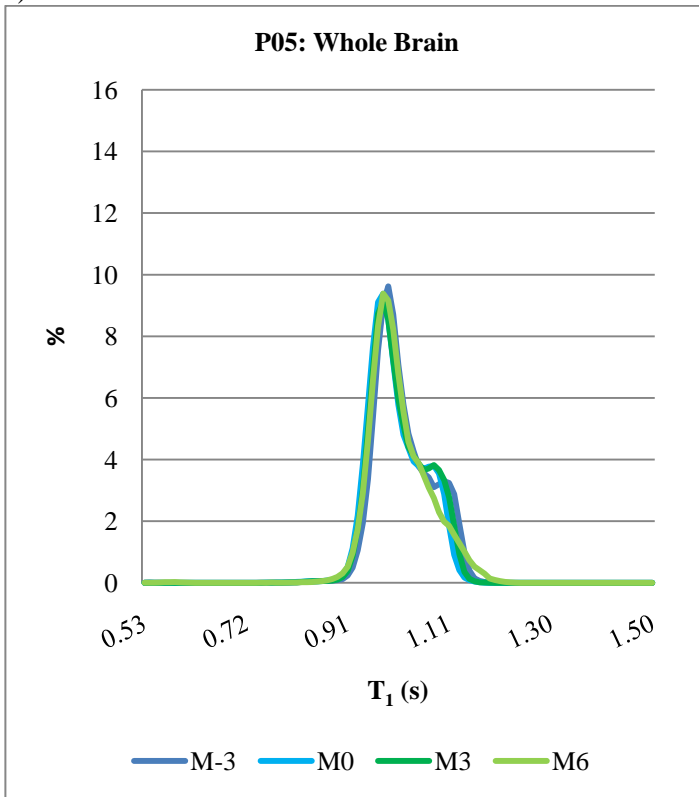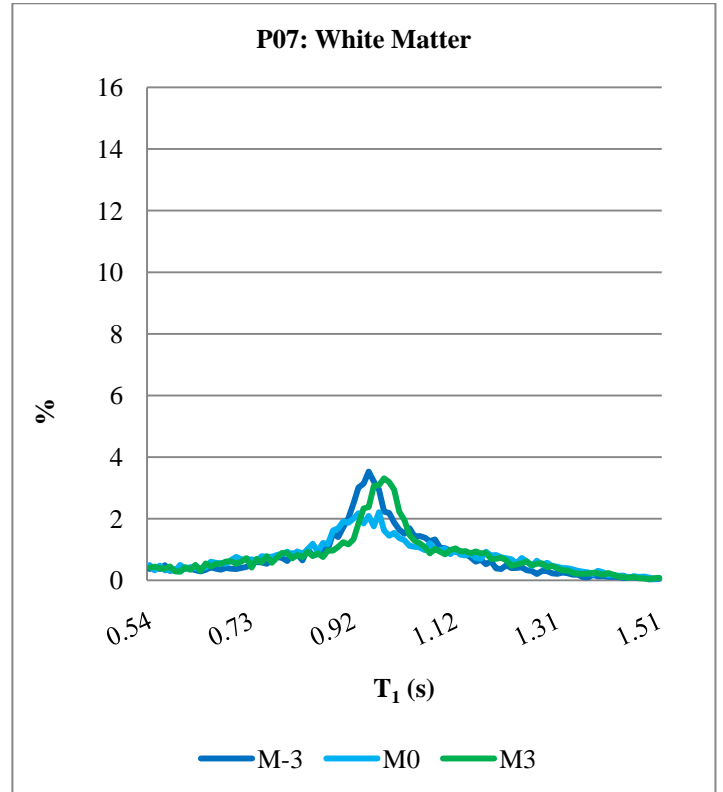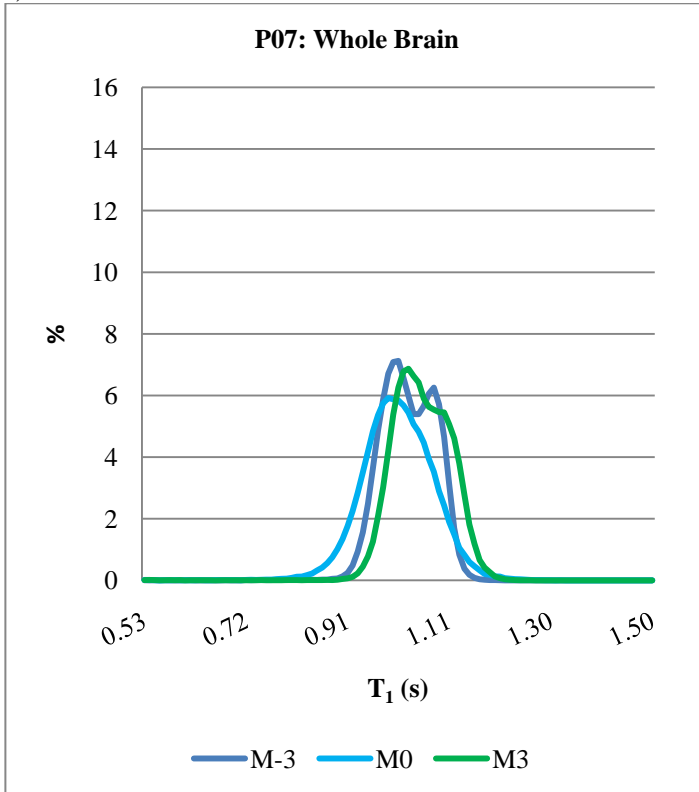
**Figure A-2 Normalized whole brain T$_1$ histograms from all subjects**

Histograms were normalized by dividing the number of pixels in each bin by the total pixel count and multiplying by 100 to obtain a percentage. Figures represent the T$_1$ histograms of individual subjects at all time point; **(a)** one to three months prior to initiating therapy; **(b)** baseline (within one week of initiating therapy); **(c)** three months after initiating therapy; **(d)** six months after initiating therapy

a)



b)
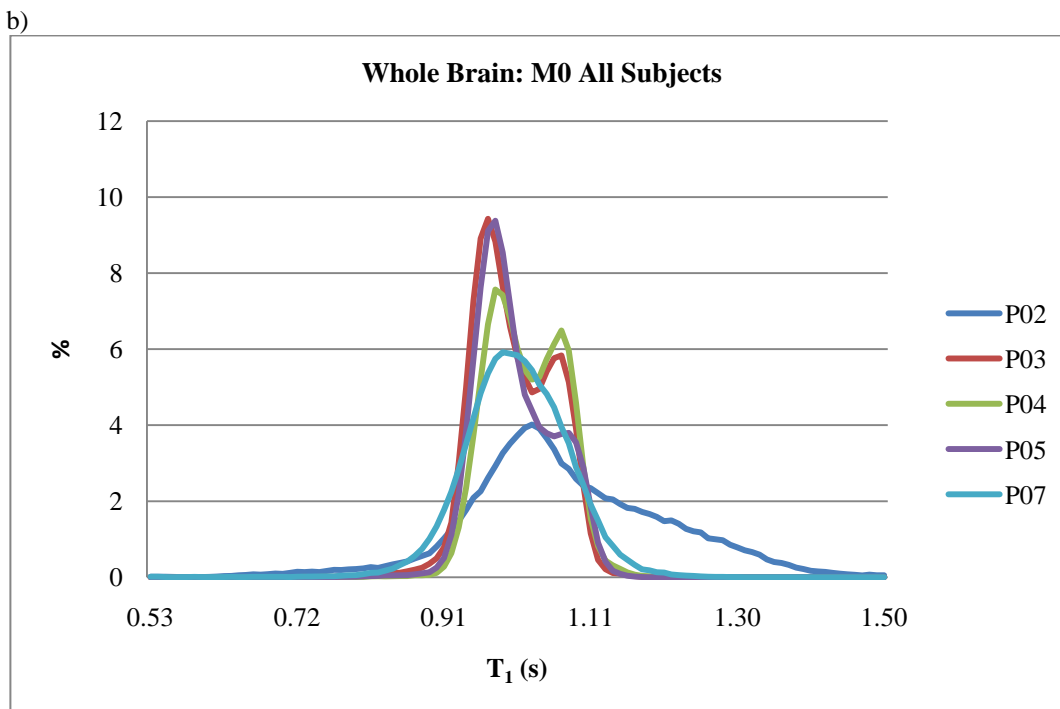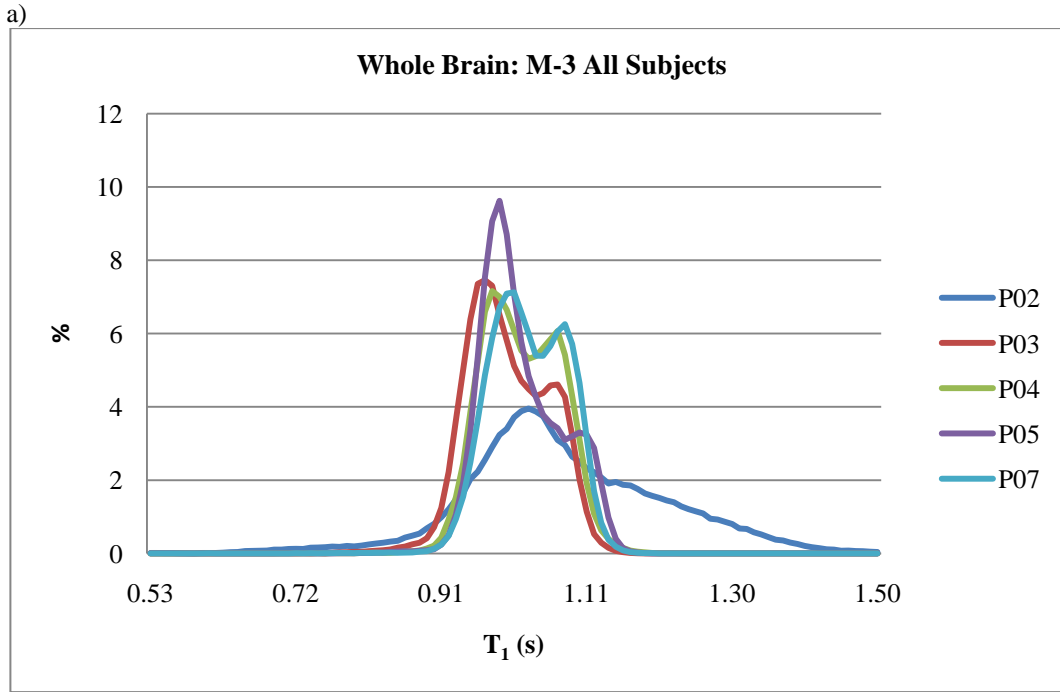
c)
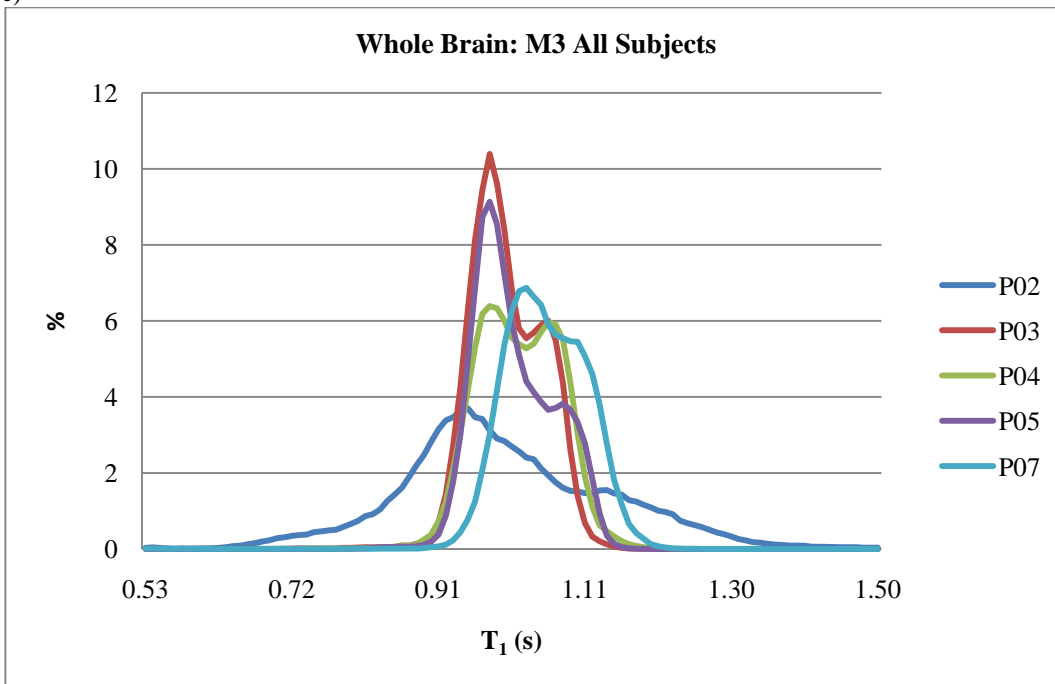


d)

# Figure A-3 Normalized white matter T$_1$ histograms from all subjects

Histograms were normalized by dividing the number of pixels in each bin by the total pixel count and multiplying by 100 to obtain a percentage. Figures represent the T$_1$ histograms of individual subjects at all time points; **(a)** one to three months prior to initiating therapy; **(b)** baseline (within one week of initiating therapy); **(c)** three months after initiating therapy; **(d)** six months after initiating therapy

a)



b)

c)



White Matter: M3 All Subjects

d)



White Matter: M6 All Subjects
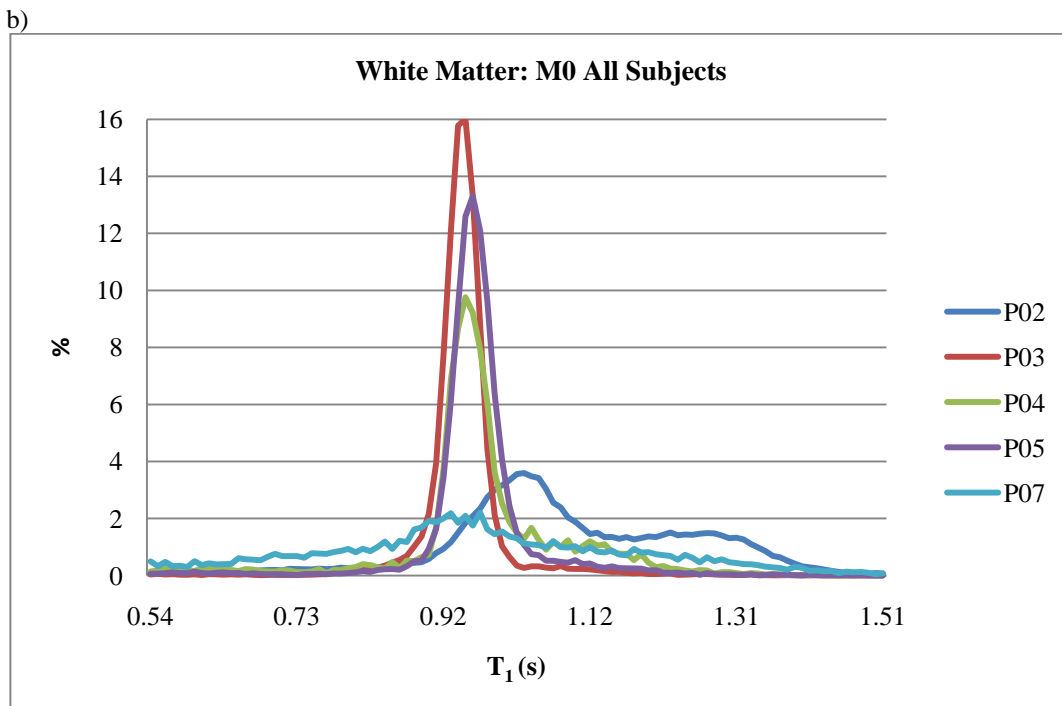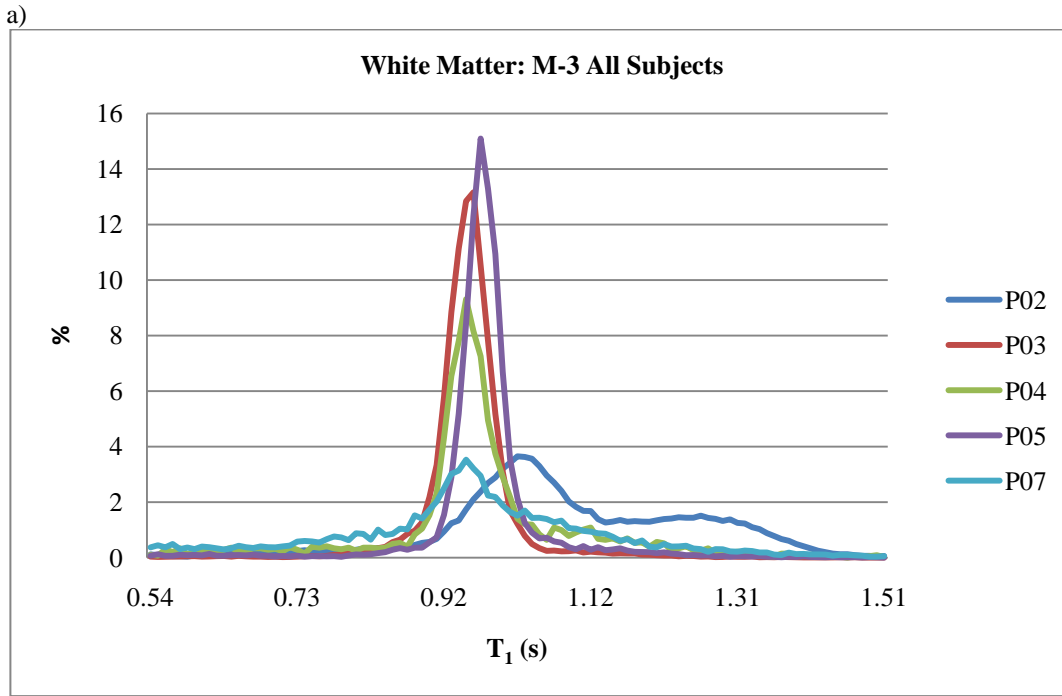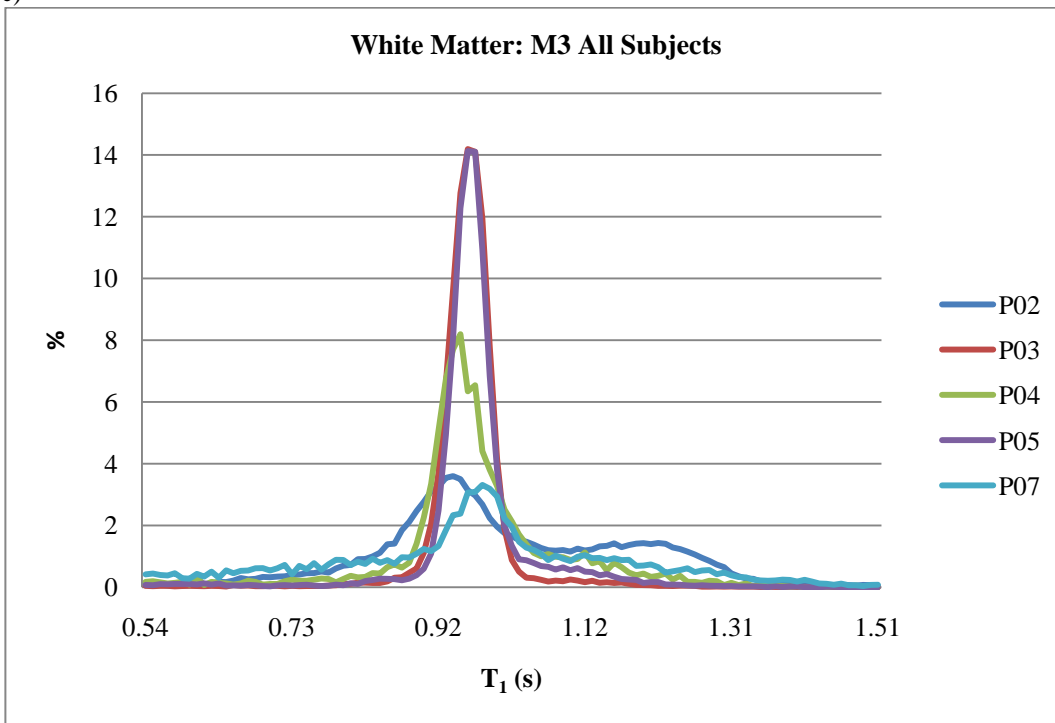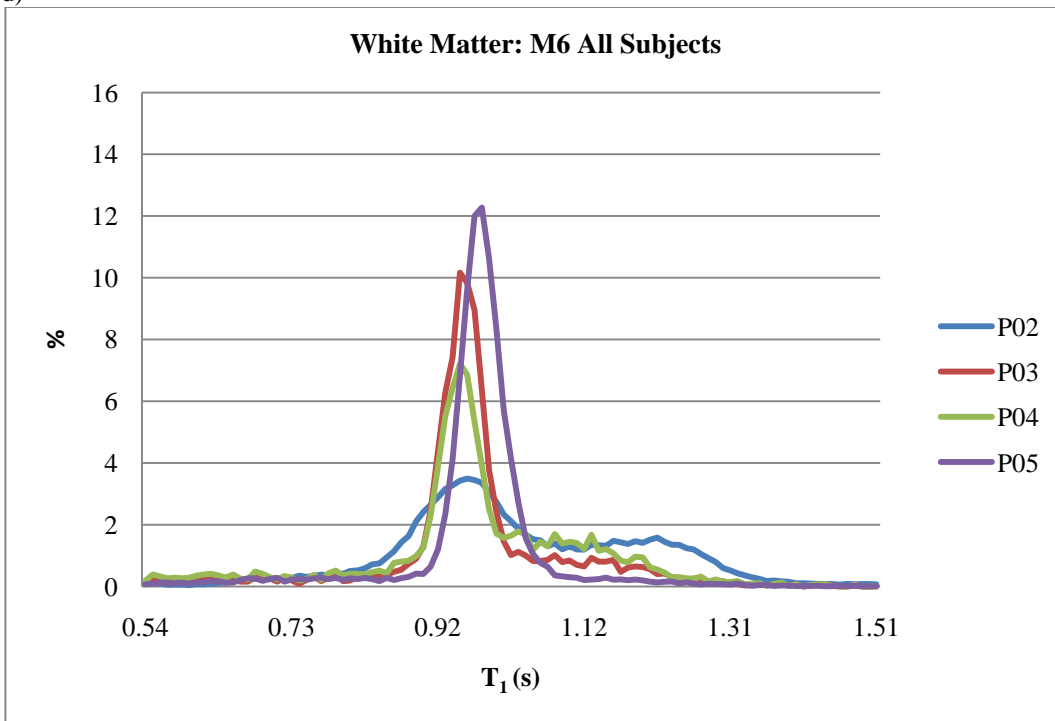
## B. Collaborations

**Identification of design and research program:** I participated in discussions where the research goals and protocol were decided upon. As well, I participated in writing of the successful Multiple Sclerosis Society of Canada Research Grant as well as a successful Multiple Sclerosis Society of Canada Research Studentship Grant.

**Performing the research:** I conducted pilot scans to test the implementation of the MRI sequence in the brain. I was also present while our subjects were scanned by the MRI technologists.

**Data analysis:** I participated in all recruitment and data collection. I performed all image registration, segmentation, data extraction and statistical analyses.

**Manuscript preparation:** I prepared the manuscript text and figures with constructive comments from all committee members and Dr. Cornelia Laule.

## C. Clinical Research Ethics Board Certificates of Approval

The University of British Columbia
Office of Research Services
Clinical Research Ethics Board – Room 210, 828 West 10th Avenue, Vancouver, BC
V5Z 1L8

# ETHICS CERTIFICATE OF EXPEDITED APPROVAL

| PRINCIPAL INVESTIGATOR: | INSTITUTION / DEPARTMENT: | UBC CREB NUMBER: |
|---|---|---|
| Anthony Traboulsee | UBC/Medicine, Faculty of/Medicine, Department of | H07-02035 |

**INSTITUTION(S) WHERE RESEARCH WILL BE CARRIED OUT:**

| Institution | Site |
|---|---|
| Vancouver Coastal Health (VCHRI/VCHA) | UBC Hospital |

Other locations where the research will be conducted:
N/A

**CO-INVESTIGATOR(S):**

Roger Tam
David K.B. Li
Alexander L. MacKay

**SPONSORING AGENCIES:**

- Multiple Sclerosis Society of Canada - "Effects of hydration status on MRI measurements of brain volume and water content"

**PROJECT TITLE:**
Pseudo-atrophy of the brain in Multiple Sclerosis

THE CURRENT UBC CREB APPROVAL FOR THIS STUDY EXPIRES: June 3, 2009

The UBC Clinical Research Ethics Board Chair or Associate Chair, has reviewed the above described research project, including associated documentation noted below, and finds the research project acceptable on ethical grounds for research involving human subjects and hereby grants approval.

| DOCUMENTS INCLUDED IN THIS APPROVAL: | | | APPROVAL DATE: |
|---|---|---|---|
| Document Name | Version | Date | |
| **Protocol:** | | | |
| Pseudo-atrophy Protocol | 3 | March 31, 2008 | |
| **Consent Forms:** | | | June 3, 2008 |
| Pseudo-Atrophy Consent Form 2 | 3 | May 23, 2008 | |
| **Letter of Initial Contact:** | | | |
| Pseudo-Atrophy Letter 2 | 3 | May 23, 2008 | |

**CERTIFICATION:**
**In respect of clinical trials:**
1. The membership of this Research Ethics Board complies with the membership requirements for Research Ethics Boards defined in Division 5 of the Food and Drug Regulations.
2. The Research Ethics Board carries out its functions in a manner consistent with Good Clinical Practices.
3. This Research Ethics Board has reviewed and approved the clinical trial protocol and informed consent form for the trial which is to be conducted by the qualified investigator named above at the specified clinical trial site. This approval and the views of this Research Ethics Board have been documented in writing.

The documentation included for the above-named project has been reviewed by the UBC CREB, and the research study, as presented in the documentation, was found to be acceptable on ethical grounds for research involving human subjects and was approved by the UBC CREB.

*Approval of the Clinical Research Ethics Board by one of:*

# ETHICS CERTIFICATE OF EXPEDITED APPROVAL: RENEWAL

| PRINCIPAL INVESTIGATOR: | DEPARTMENT: | UBC CREB NUMBER: |
|---|---|---|
| Anthony Traboulsee | UBC/Medicine, Faculty of/Medicine, Department of | H07-02036 |

**INSTITUTION(S) WHERE RESEARCH WILL BE CARRIED OUT:**

| Institution | Site |
|---|---|
| Vancouver Coastal Health (VCHRI/VCHA) | UBC Hospital |

Other locations where the research will be conducted:
N/A

**CO-INVESTIGATOR(S):**
Roger Tam
David K.B. Li
Alexander L. MacKay

**SPONSORING AGENCIES:**
- Multiple Sclerosis Society of Canada - "Effects of hydration status on MRI measurements of brain volume and water content"

**PROJECT TITLE:**
Pseudo-atrophy of the brain in Multiple Sclerosis

**EXPIRY DATE OF THIS APPROVAL:  June 15, 2010**

**APPROVAL DATE:   June 15, 2009**

**CERTIFICATION:**
**In respect of clinical trials:**
1. The membership of this Research Ethics Board complies with the membership requirements for Research Ethics Boards defined in Division 5 of the Food and Drug Regulations.
2. The Research Ethics Board carries out its functions in a manner consistent with Good Clinical Practices.
3. This Research Ethics Board has reviewed and approved the clinical trial protocol and informed consent form for the trial which is to be conducted by the qualified investigator named above at the specified clinical trial site. This approval and the views of this Research Ethics Board have been documented in writing.

The Chair of the UBC Clinical Research Ethics Board has reviewed the documentation for the above named project. The research study, as presented in the documentation, was found to be acceptable on ethical grounds for research involving human subjects and was approved for renewal by the UBC Clinical Research Ethics Board.

*Approval of the Clinical Research Ethics Board by one of:*